OXFORD GENETICS

GENETICS, 2022, 222(1), iyac105
https://doi.org/10.1093/genetics/iyac105
Advance Access Publication Date: 25 July 2022
Investigation

A distinct P-body-like granule is induced in response to the disruption of microtubule integrity in *Saccharomyces cerevisiae*

Zachary Hurst ,† Wenfang Liu ,† Qian Shi , Paul K. Herman *

Department of Molecular Genetics, The Ohio State University, Columbus, OH 43210, USA

*Corresponding author: Department of Molecular Genetics, The Ohio State University, 484 W. 12th Ave., Rm. 105, Columbus, OH 43210, USA.
Email: herman.81@osu.edu
†These authors contributed equally to this work.

Abstract

The Processing-body is a conserved membraneless organelle that has been implicated in the storage and/or decay of mRNAs. Although Processing-bodies have been shown to be induced by a variety of conditions, the mechanisms controlling their assembly and their precise physiological roles in eukaryotic cells are still being worked out. In this study, we find that a distinct subtype of Processing-body is induced in response to conditions that disrupt microtubule integrity in the budding yeast, *Saccharomyces cerevisiae*. For example, treatment with the microtubule-destabilizing agent, benomyl, led to the induction of these novel ribonucleoprotein granules. A link to microtubules had been noted previously and the observations here extend our understanding by demonstrating that the induced foci differ from traditional P-bodies in a number of significant ways. These include differences in overall granule morphology, protein composition, and the manner in which their induction is regulated. Of particular note, several key Processing-body constituents are absent from these benomyl-induced granules, including the Pat1 protein that is normally required for efficient Processing-body assembly. However, these novel ribonucleoprotein structures still contain many known Processing-body proteins and exhibit similar hallmarks of a liquid-like compartment. In all, the data suggest that the disruption of microtubule integrity leads to the formation of a novel type of Processing-body granule that may have distinct biological activities in the cell. Future work will aim to identify the biological activities of these benomyl-induced granules and to determine, in turn, whether these Processing-body-like granules have any role in the regulation of microtubule dynamics.

Keywords: ribonucleoprotein (RNP) granules; Processing-bodies; microtubules; prefoldin; liquid-liquid phase separation; casein kinase I

Introduction

The interior of the eukaryotic cell is divided into functionally distinct areas by the presence of both membrane-bound and membraneless compartments. Although many of the latter have only been recognized recently, several including the nucleolus have been studied for decades (Ho *et al.* 2002; Boisvert *et al.* 2007; Brangwynne *et al.* 2011; Hyman *et al.* 2014). These membraneless structures are known by a variety of names including biomolecular condensates and membraneless organelles (Hyman *et al.* 2014; Toretsky and Wright 2014; Banani *et al.* 2017; Boeynaems *et al.* 2018). These condensates lack a limiting membrane and are typically dynamic entities that can assemble rapidly in response to the appropriate cues. Many of these compartments have been shown to exhibit liquid-like behavior and are thought to form as a result of a phase transition known as liquid-liquid phase separation (Li *et al.* 2012; Hyman *et al.* 2014; Alberti 2017; Banani *et al.* 2017; Boeynaems *et al.* 2018). Recent work indicates that condensate formation is important for many fundamental processes in the cell, including RNA polymerase II transcription (Boehning *et al.* 2018; Leblanc *et al.* 2021; Rippe and Papantonis 2022). Understanding how the assembly and function of these structures are regulated is therefore key for a complete description of eukaryotic biology.

One family of biomolecular condensates is made up of a collection of cytoplasmic granules that contain distinct sets of proteins and mRNAs. The Processing-body, or P-body, is one such ribonucleoprotein (RNP) granule that has been conserved from yeasts to mammals (Eulalio *et al.* 2007; Parker and Sheth 2007; Franks and Lykke-Andersen 2008; Anderson and Kedersha 2009). The P-body was originally identified as an RNP structure that contains proteins involved in the processing and decay of mRNAs (Bashkirov *et al.* 1997; Ingelfinger *et al.* 2002; van Dijk *et al.* 2002; Eystathioy *et al.* 2003; Sheth and Parker 2003; Cougot *et al.* 2004; Xing *et al.* 2020). These proteins include the Xrn1 exonuclease and the Dcp1/Dcp2 decapping complex. As a result, it was initially proposed that P-body foci were sites of active mRNA decay in the cytoplasm (Stoecklin *et al.* 2006; Eulalio *et al.* 2007; Balagopal and Parker 2009). However, more recent data indicate that mRNAs may be stored long term in P-bodies and that mRNA decay might even be suppressed within these granules (Arribere

Received: June 09, 2022. **Accepted:** July 08, 2022

et al. 2011; Zid and O'Shea 2014; Hubstenberger et al. 2017; Huch and Nissan 2017; Standart and Weil 2018). Ongoing efforts aim to determine how these decay enzymes are regulated within the P-body and to identify the precise physiological roles of this RNP granule. Some insight into the latter has been provided by studies demonstrating that P-bodies contain proteins involved in other aspects of cell physiology, including signal transduction (Shah et al. 2014). These and other studies in yeast have identified critical roles for P-bodies during the early stages of meiosis, in response to replicative and cell wall stresses, and for the long-term survival of quiescent cells (Ramachandran et al. 2011; Shah et al. 2013; Zhang et al. 2016; Loll-Krippleber and Brown 2017; Zhang et al. 2018; García et al. 2019). However, it is not yet clear whether these effects are due to an influence on mRNA stability and/or other activities that may be associated with these RNP granules.

The maintenance of proper protein homeostasis, or proteostasis, is necessary for essentially all physiological processes in the cell. Proteostasis involves an extensive network of components that ensure that proteins are present at their appropriate conformation, concentration, and cellular location. Proteins that fail to fold properly will interact with this network and will be either refolded, degraded or sequestered at particular sites within the cell (Hartl et al. 2011; Sontag et al. 2017). Proteins that assist in the folding process are referred to as chaperones and eukaryotic cells contain a significant variety of such activities. A particular folding pathway of note for this study involves the prefoldin and Cct/chaperonin complexes (Martín-Benito et al. 2002; Gestaut et al. 2019). Prefoldin is an ATP-independent chaperone that functions in part by delivering unfolded protein substrates to the Cct/chaperonin complex (Vainberg et al. 1998; Gestaut et al. 2019). The latter is a conserved, 8-subunit complex that utilizes ATP hydrolysis to promote proper protein folding (Thirumalai and Lorimer 2001). Although prefoldin has many substrates, two of the best characterized are the α- and β-tubulin monomers used to construct the cellular microtubule networks (Vainberg et al. 1998; Martín-Benito et al. 2002). Following their release from the Cct/chaperonin complex, these tubulin monomers are acted upon by a series of additional tubulin-specific chaperones that facilitate the formation of the α/β heterodimer (Lewis et al. 1997; Lopez-Fanarraga et al. 2001; Szymanski 2002). This final heterodimer can then be incorporated into the existing microtubule polymers present in the cell.

Studies with the budding yeast, *Saccharomyces cerevisiae*, have identified several proteins, including Pat1, that are critical for the formation of the P-body (Teixeira and Parker 2007; Pilkington and Parker 2008; Braun et al. 2010; Marnef and Standart 2010). Pat1 is a conserved core constituent of these granules and a key target of control during the assembly process. For example, the phosphorylation of Pat1 by the cAMP-dependent kinase (PKA) inhibits P-body formation perhaps by preventing specific interactions with other granule components (Ramachandran et al. 2011; Sachdev et al. 2019). Yeast cells lacking Pat1 exhibit a significant defect in P-body assembly. Here, we used a genetic approach to gain insight into the P-body assembly process by identifying second-site suppressors of this *pat1*Δ defect. Interestingly, mutations disrupting the prefoldin-Cct/chaperonin pathway were found to restore P-body formation in *pat1*Δ mutants. The data further indicate that this suppression is likely due to effects on the microtubule network and that the disruption of this network results in the formation of P-body-like granules even in wild-type cells. Previous work has suggested a connection between P-bodies and microtubules and the studies here extend these observations by demonstrating that the granules formed differ significantly from the traditional P-bodies induced by other stress conditions, like glucose deprivation (Sweet et al. 2007). The significance of these differences for P-body assembly and function are discussed.

Materials and methods

Yeast strains and growth conditions

All yeast strains used in this study were generated using standard methods and are listed in Supplementary Table 1. Unless otherwise noted, the wild-type (*wt*) strain for the experiments presented was BY4741. The prefoldin (*PFD*) and tubulin folding cofactor (TFC) deletion strains were obtained from the yeast knockout collection (Open Biosystems). Strains expressing GFP-protein fusion constructs were obtained from the yeast GFP collection (Invitrogen). The *pfd*Δ *pat1*Δ and *tfc*Δ *pat1*Δ double mutants were generated by replacing the coding sequences of the *PAT1* locus with the *LEU2* gene. The *edc3*Δ *lsm4*Δ*C* strain was generated by replacing the 3′-end of the *LSM4* gene that encodes the C-terminal half of the Lsm4 protein with the *LEU2* gene, as described previously (Decker et al. 2007). The *pfd1*Δ *edc3*Δ *lsm4*Δ*C* strain was generated by replacing the coding sequence of *PFD1* with the *URA3* gene. C-terminal fluorescent protein fusion constructs with the different P-body proteins were generated with a PCR-based recombination strategy as described previously (Huh et al. 2003). The temperature-sensitive *cct4-1* and *cct6-18* strains from the Charles Boone *ts* strain collection were generously provided by Dr. Anita Hopper (Li et al. 2011).

Standard *Escherichia coli* and yeast culture methods were employed throughout this study. Yeast strains were cultivated in yeast extract–peptone–adenine–dextrose (YPAD) or synthetic complete drop-out media lacking the appropriate amino acids and supplemented with 2% dextrose (SCD) at 30°C. Yeast transformations were accomplished with a standard lithium acetate/polyethylene-glycol protocol (Gietz and Schiestl 2007).

Plasmid construction

The plasmids used in this study are listed in Supplementary Table 2. All genes, unless explicitly stated to the contrary, are expressed from their endogenous promoters.

Drug treatment of yeast cultures

Benomyl treatment

A 10 mg/ml stock solution of benomyl [methyl 1-(butylcarbamoyl)-2-benzimidazolecarbamate, Sigma-Aldrich] was prepared in DMSO and sterilized by passage through a 0.2-μm syringe filter. Media containing benomyl were prepared fresh on the day of the experiment. The benomyl stock solution was added dropwise to prewarmed culture media with continuous stirring to ensure complete dissolution. Cell cultures were grown to mid-log phase in the appropriate medium, collected by centrifugation, and resuspended in fresh medium containing benomyl (or DMSO) at the concentration indicated for each experiment.

Latrunculin A treatment

A 2 mM stock solution of latrunculin A (Sigma-Aldrich) was prepared in DMSO and sterilized by passage through a 0.2-μm syringe filter. Cell cultures were grown to mid-log phase in SCD medium, collected by centrifugation, and resuspended in fresh medium containing 200 μM latrunculin A for 30 min to disrupt the actin cytoskeleton (Sahin et al. 2008).

1,6-Hexanediol treatment

A 50% stock solution of 1,6-hexanediol (Sigma-Aldrich) was prepared by dissolving 1,6-hexanediol crystals in water and sterilized by passage through a 0.2-μm filter. The appropriate yeast cells were grown to mid-log phase and subjected to either glucose starvation for 30 min or treatment with benomyl to induce foci formation. Following this induction, 1,6-hexanediol was added to a final concentration of 10% (v/v) for 10 min.

Fluorescent microscopy and image quantification

Cells expressing fluorescently labeled fusion protein constructs were grown as indicated, collected by centrifugation, and spotted onto agarose pads affixed to microscope slides as described previously (Shah *et al.* 2013; Zhang *et al.* 2016). Cells were imaged with a ×100/1.45 numerical aperture Plan-Apo objective lens on a Nikon Eclipse Ti inverted microscope (Nikon) with an Andor Zyla sCMOS 4.2 MP digital camera. Appropriate Nikon HC filter sets were used for each fluorescent channel. For each experiment, identical exposure times and acquisition conditions were utilized to permit direct comparison of pixel intensities between images acquired both within the same experiment and for the same fluorescent reporter construct. The scale bar depicted in the bottom right-most image in each figure represents 5 μm. Image postprocessing was performed using the Fiji ImageJ (NIH) software package. All images within a given experiment and for a given fluorescent reporter construct were subjected to an identical postprocessing regimen with respect to brightness and contrast adjustments. Where indicated, a maximum intensity z-projection was generated from a z-stack of serial images acquired for the same field-of-view using a slice interval of 0.2 μm.

When quantifying the percentage of cells containing foci, the data presented in this study represent a minimum of 2 independent experimental replicates with >100 cells examined for each condition in each replicate. Where provided, the percentage of cells containing foci represent the average for a particular experimental condition across all experimental replicates. Due to the morphological differences between benomyl-induced granules (BIGs) and glucose starvation-induced P-bodies, a fluorescent intensity thresholding method was applied to increase objectivity in defining a bona fide focus. First, the LUT histograms for all images acquired for the same fluorescent reporter construct within the same experiment were normalized. Second, a baseline intensity threshold, defined as the intensity at which only pixels containing foci were observable, was assessed individually for each fluorescent reporter construct during mid-log phase growth (the control growth condition). This baseline intensity threshold was then applied to the images acquired for cells subjected to the various experimental conditions outlined in this study. In doing so, only cells that contained foci of equal or greater intensity to that of the control, the mid-log phase condition, were counted as "foci containing cells."

Evaluation of colocalization between fluorescent reporter constructs was conducted with two methodologies. First, the percentage of colocalization between two fluorescent reporters was calculated by scoring the proportion of foci which demonstrated coincidence between the two fluorescent channels only in those cells possessing at least one focus for both reporters. Consequently, cells which possessed foci for only one reporter were excluded. Second, the Pearson's, Mander's, and Li's colocalization coefficients were assessed for the indicated fluorescent reporter constructs using the Fiji Plugin JACoP (**J**ust **A**nother **Co**localization **P**lugin) (Manders *et al.* 1992; Li *et al.* 2004; Bolte and Cordelières 2006).

A two-proportion *Z*-test was used to assess the statistical significance of the relevant data in this report. The resultant *P*-values for all the pair-wise comparisons made are included in Supplementary Table 3. The raw data for these analyses are available upon request.

Protein analysis

Protein samples were prepared for western blotting using a glass bead lysis method (Budovskaya *et al.* 2002; DeCaprio and Kohl 2020). A Bradford assay was performed to quantify the total protein in the lysates and equivalent quantities of protein were loaded per gel well. Protein samples were resolved on an 8% SDS-polyacrylamide gel, transferred to a nitrocellulose membrane, and probed with the appropriate primary and secondary antibodies. The results were then visualized using fluorescent detection with the LiCOR Odyssey Imaging System. The primary antibodies used were mouse anti-Myc-Tag (1:2,000 dilution, # 2276S; Cell Signaling Technologies), mouse anti-GFP (1:2,000 dilution, # MA5-15256; Invitrogen), and rabbit anti-Pgk1 (1:20,000 dilution, kindly provided to our lab by Dr. Jeremy Thorner). The secondary antibodies used were IRDye-680RD donkey anti-rabbit (1:10,000 dilution, # 926-68073; Li-COR), IRDye-800CW goat anti-rat (1:10,000 dilution, # 926-32219; Li-COR), and IRDye-800CW goat anti-mouse (1:10,000 dilution, # 926-32210; Li-COR).

Extracts for the coimmunoprecipitation studies were prepared by resuspending cells in lysis buffer (25 mM Tris-HCl, pH 7.4, 140 mM NaCl, 0.05% Tween-20, 1 mM PMSF) and then agitating with glass beads, as described (Deminoff *et al.* 2009; Zhang *et al.* 2016). TAP-tagged proteins were immunoprecipitated with Protein A Dynabeads (# 10001D; Invitrogen). Protease and phosphatase inhibitors were present at all steps. The extent of interaction was then assessed by western blotting with the rabbit anti-Tap antibody (1:2,000 dilution, # CAB1001; Invitrogen) and rat anti-Tubulin antibody (1:4,000 dilution, # ab6161; Abcam).

Assessing relative PKA levels with the Cki1 reporter construct

The Cki1 reporter ($CUP1_{pro}$-6X Myc-$Cki1^{1-200}$) was expressed from the plasmid, pPHY2328, and used to assess the relative level of in vivo PKA activity as described previously (Deminoff *et al.* 2006; Ramachandran and Herman 2011). Strains harboring the Cki1 reporter construct were grown to an OD_{600} of 0.3 units/ml in SCD medium. $CuSO_4$ was added to a final concentration of 100 μM, and the strains were incubated for an additional 2 h to induce expression of the reporter construct. After induction, strains were subjected to either a glucose starvation or benomyl treatment for 1 h. The cells were then collected by centrifugation and protein extracts were prepared for western blotting as described above. Quantification of the ratio of phosphorylated to nonphosphorylated Cki1 (Cki1-P*/Cki1) was performed using the LiCOR ImageStudio software package.

Spotting assay to assess benomyl sensitivity

Yeast strains were grown to mid-log phase and cells were collected by centrifugation. All strains were then resuspended in water at a final concentration of 5 OD_{600} equivalents/ml. Five-fold serial dilutions were prepared from this suspension and 5 μl of each dilution were spotted in succession onto plates containing the appropriate growth media, with and without benomyl at the concentration(s) indicated. The plates were photographed after incubation at 30°C for 2–3 days.

Characterization of the Tub1- and Tub3-GFP fusion constructs

Genomic DNA was extracted from both the Tub1-GFP and Tub3-GFP strains obtained from the GFP collection (Invitrogen). A genotyping PCR was performed to amplify the relevant chromosomally integrated GFP fusion constructs from the gDNA templates. The forward primers were specific to sequences within the 5′-UTRs of the *TUB1* and *TUB3* loci, respectively, and the reverse primers to sequences within the GFP coding region. While no amplicon resulted from the Tub1-GFP-specific primer set in either strain, an amplicon resulting from the Tub3-GFP-specific primer set was observed in both strains. These amplicons were subsequently sequenced (OSU Genomic CORE) using primers flanking the *TUB1* and *TUB3* coding sequences. Sequence alignment to the *TUB3* coding sequence indicated that the "Tub1-GFP" strain encoded an unusual variant of Tub3 fused to GFP. This fusion most likely resulted from the recombination of a fragment containing homology to the 3′-end of *TUB1* at the corresponding end of the *TUB3* gene. This resulted in the formation of a Tub3Δ-Tub1$_{C\text{-}term}$-GFP hybrid construct (see Supplementary Fig. 6a). Further sequencing confirmed that in this "Tub1-GFP" strain, the GFP::*hisMX3* cassette with *TUB1* homology was not successfully recombined into the *TUB1* locus.

Results

P-body-like granules were present in cells defective for prefoldin function

Yeast cells lacking the Pat1 protein are defective for P-body assembly (Fig. 1a) (Coller and Parker 2005; Pilkington and Parker 2008; Ramachandran *et al.* 2011). We found that this defect was partially suppressed by the loss of the *PFD1* gene that encodes one of the subunits of the heterohexameric prefoldin complex (Geissler *et al.* 1998; Martín-Benito *et al.* 2002). The fraction of cells containing a P-body focus was higher in the *pfd1*Δ *pat1*Δ double mutant than in the *pat1*Δ strain (Fig. 1a and Supplementary Fig. 1). P-body formation was assessed by examining the localization of Dcp2, Edc3 and Dhh1, three core constituents of P-body granules, after a period of glucose deprivation. Although prefoldin is thought to act primarily in protein quality control, there are reports suggesting that noncanonical subcomplexes of prefoldin subunits have different functions in the cell (Millán-Zambrano *et al.* 2013; Millán-Zambrano and Chávez 2014; Liang *et al.* 2020). Therefore, we tested whether the suppression of the *pat1*Δ defect was observed with strains containing single deletions of the remaining five *PFD* genes. Previous work has demonstrated that prefoldin function is largely lost in cells lacking any of the six subunits (Miyazawa *et al.* 2011). We found that the *pat1*Δ defect was suppressed to a similar extent by the deletion of any one of the six *PFD* genes (Fig. 1b). The fraction of cells containing a higher intensity focus was typically 5- to 8-times greater in the *pfd*Δ *pat1*Δ double mutants relative to the *pat1*Δ strain (Supplementary Fig. 2, a and b). Altogether, these data suggested that the suppression of the *pat1*Δ defect was due to the loss of prefoldin chaperone activity.

We also tested whether the loss of prefoldin function would restore P-bodies in a second mutant defective for granule formation. This *edc3*Δ *lsm4*ΔC strain has alterations at two loci, *EDC3* and *LSM4*. Edc3 is a component of P-bodies that has been shown to act as an enhancer of mRNA decapping (Kshirsagar and Parker 2004; Nissan *et al.* 2010). Lsm4 is an essential protein that is a constituent of the Lsm1–7 and Lsm2–8 heptameric protein complexes. The former is required for the 5′-to-3′ degradation of mRNAs and is found in the cytoplasm and within P-body granules (Bouveret *et al.* 2000; Ingelfinger *et al.* 2002; Beggs 2005). The latter is localized to the nucleus and is involved in mRNA splicing (Séraphin 1995; Beggs 2005; Novotny *et al.* 2012). The *lsm4*ΔC allele encodes a truncated protein that lacks a C-terminal domain predicted to be intrinsically disordered (Decker *et al.* 2007; Reijns *et al.* 2008; Oishi *et al.* 2013; Huch *et al.* 2016). Cells with both the *edc3*Δ and *lsm4*ΔC mutations exhibit a significant defect in P-body formation (Fig. 1c) (Decker *et al.* 2007; Reijns *et al.* 2008). However, deletion of the *PFD* genes did not suppress this P-body assembly defect; results for the *pfd1*Δ *edc3*Δ *lsm4*ΔC mutant are shown in Fig. 1c. Moreover, we did not observe any suppression of the *pat1*Δ defect with the other chaperone gene deletions examined, including *hsp26*Δ, *hsp42*Δ, and *hsp104*Δ (data not shown). Thus, the suppression by the *pfd*Δ mutations was specific for the P-body defect conferred by the loss of the *PAT1* locus.

While examining the *pfd1*Δ strain, we noted that Dcp2- and Edc3-containing foci were also present in glucose-replete conditions (Fig. 2a). Similar results were obtained for both reporters with the other *pfd*Δ mutants (Fig. 2, b and c). Upon glucose deprivation, the number of *pfd*Δ cells containing P-body foci increased to a value that was similar or slightly less than that observed with the wild-type control (Fig. 2, b and c). Therefore, P-body-like granules were present constitutively in strains lacking prefoldin function.

As prefoldin acts in concert with the Cct/chaperonin complex, we also tested whether P-body-like granules were present in cells lacking this latter chaperone activity. Since the Cct/chaperonin complex is essential for *S. cerevisiae* viability, conditional alleles of the *CCT4* and *CCT6* genes were used for these studies (Ursic and Culbertson 1991; Grantham *et al.* 2006). Both alleles, *cct4-1* and *cct6-18*, encode temperature-sensitive products that are inactivated upon a shift to 37°C (Li *et al.* 2011). We found that a short exposure to this elevated temperature in glucose-replete conditions led to an increase in both Dcp2- and Edc3-containing foci in these mutant strains (Fig. 2d). The results with Pat1 will be discussed below. Thus, the loss of Cct/chaperonin activity also resulted in elevated granule formation. It should be noted that elevated levels of foci were constitutively present when these *cct*^{ts} strains were grown at the semi-permissive temperature of 30°C. This effect was most pronounced for the Edc3 reporter (Fig. 2d). The permissive temperature for these experiments was 25°C. This result was similar to what was seen with the *pfd*Δ mutants where P-body-like foci were also present constitutively. Altogether, these data suggested that the P-body induction described here was due to the misfolding of specific targets of the prefoldin-Cct/chaperonin pathway.

Tubulin monomers are the likely prefoldin substrates responsible for the elevated formation of P-body-like foci

Previous work indicates that there are many substrates for the prefoldin complex in vivo (Geissler *et al.* 1998; Vainberg *et al.* 1998). Perhaps the best characterized of these are the actin and tubulin monomers that make up two of the key cytoskeletal systems in the eukaryotic cell (Simons *et al.* 2004). Here, we tested whether disruption of either of these networks would also suppress the P-body assembly defect of the *pat1*Δ mutant. The drugs, latrunculin A and benomyl, were used to disrupt the actin and microtubule networks, respectively (Machin *et al.* 1995; Richards *et al.* 2000; Cox *et al.* 2004; Sahin *et al.* 2008). The growth of *pfd*Δ mutants has been shown to be sensitive to both of these

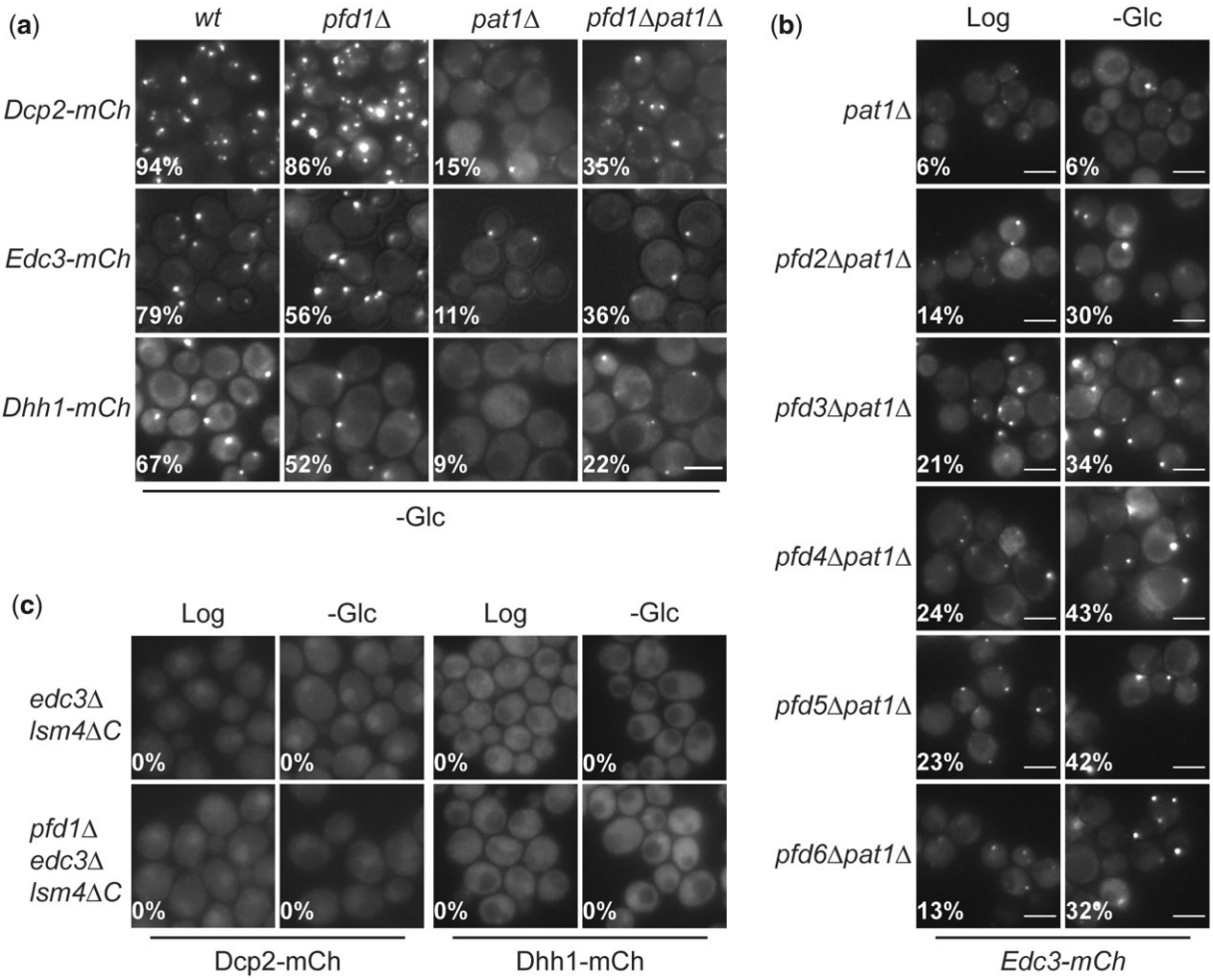

Fig. 1. The loss of prefoldin chaperone activity suppressed the P-body assembly defect associated with the *pat1*Δ mutant. a, b) Deletion of any of the six *PFD* genes resulted in the suppression of the *pat1*Δ P-body formation defect. Cells expressing the indicated P-body reporters were grown to mid-log phase and then transferred to a medium lacking glucose for 30 min. The cells were examined by fluorescence microscopy both before (Log) and after the period of glucose deprivation (−Glc). The fraction of cells with a visible focus is indicated. Scale bar, 5 μm. c) Deletion of *PFD1* did not suppress the P-body formation defect of the *edc3*Δ *lsm4*Δ*C* mutant. Cells expressing the indicated P-body reporters were analyzed as described in (a). The observed differences in foci formation were determined to be statistically significant with a two-proportion Z-test where the resultant *P*-values were all less than 7×10^{-7}. The *P*-values for all relevant comparisons are provided in Supplementary Table 3.

inhibitors (Vainberg *et al.* 1998). It is important to note that the loss of any of the six *PFD* genes resulted in a similar sensitivity to benomyl (Supplementary Fig. 3a). This result conflicts with an earlier report suggesting that the *pfd1*Δ mutant did not exhibit this sensitivity (Millán-Zambrano *et al.* 2013). Here, we found that the *pat1*Δ defect was suppressed by the presence of benomyl but not latrunculin A (Fig. 3a and Supplementary Fig. 3b). For these studies, *pat1*Δ cells were transferred to a medium lacking glucose and containing the appropriate drug. The level of suppression with benomyl was similar to that observed with the *pfd*Δ mutations. This effect was again largely specific for the *pat1*Δ strain as there was little suppression by benomyl noted with the *edc3*Δ *lsm4*Δ*C* mutant (Fig. 3b). Therefore, the *pfd*Δ-mediated suppression of the *pat1*Δ defect may be due to effects on the microtubule system.

A potential connection between P-bodies and microtubules has been reported previously. Studies with both yeast and mammalian cells have found that P-body numbers can increase in response to treatments that disrupt microtubules (Sweet *et al.* 2007; Aizer *et al.* 2008). It has also been reported that P-body granules may move along microtubule networks in mammalian cells (Aizer *et al.* 2008). Here, we set out to confirm and extend these observations. We first tested whether the addition of benomyl would trigger P-body formation in log-phase cultures of wild-type yeast cells. Such a result would be consistent with the constitutive presence of P-body-like granules in the *pfd*Δ strains. Indeed, we found that P-body-like foci were induced following a 60-min treatment with benomyl (Fig. 3c). The benomyl concentration used, 15 μg/ml, did not have a significant effect on the growth of wild-type cells (Supplementary Fig. 3a). Multiple P-body reporters were found within these granules, including Dcp1, Dcp2, Edc3, Lsm1, and Xrn1 (Fig. 3c). This induction was specific for P-bodies as the presence of benomyl did not lead to the formation of a second RNP granule, known as the stress granule (Supplementary Fig. 3c). Stress granule formation was assessed by the visualization of the Pab1, Pbp1, and Pub1 reporters (Swisher and Parker 2010; Kozubowski *et al.* 2011; Kroschwald *et al.* 2018). Finally, the addition of latrunculin A to wild-type cells did not result in the

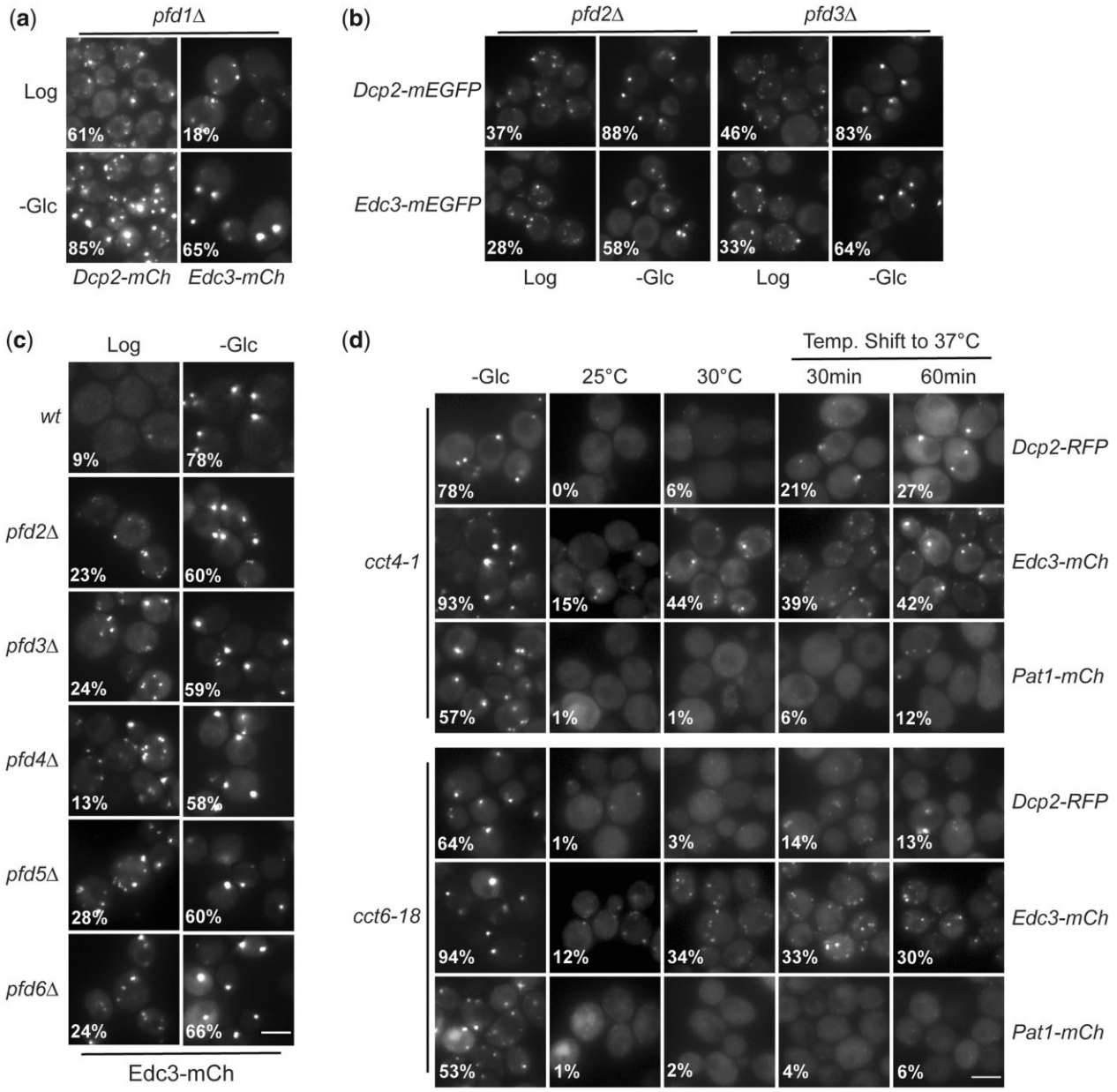

Fig. 2. The loss of prefoldin or Cct/chaperonin activity resulted in the constitutive induction of P-body-like foci. a–c) Deletion of any of the six *PFD* genes resulted in the presence of P-body-like foci during log phase growth. Cells expressing either the Dcp2- or Edc3-mCh reporter were grown to mid-log phase and then transferred to a medium lacking glucose for 30 min. The cells were examined by fluorescence microscopy both before (Log) and after the period of glucose deprivation (−Glc). The fraction of cells with a visible focus is indicated. d) The loss of Cct/chaperonin activity led to the induction of P-body-like granules. Strains harboring the temperature-sensitive alleles, *cct4-1* and *cct6-18*, were examined by fluorescence microscopy after growth at 25°C (permissive temperature), 30°C (semipermissive) or following a temperature shift from 25°C to 37°C (nonpermissive) for 30 or 60 min. The fraction of cells with a visible focus is indicated for each condition. Scale bar, 5 μm. The observed differences in foci formation were determined to be statistically significant with a two-proportion Z-test where the resultant *P*-values were typically less than 2×10^{-6}. The *P*-values for all relevant comparisons are provided in Supplementary Table 3.

formation of these P-body-like granules (Supplementary Fig. 3d). Thus, disruption of the microtubule network appeared to lead to a specific induction of P-body-like foci.

We further examined the effects of perturbing microtubule integrity by assessing P-body formation in strains defective for a set of tubulin-specific chaperones. Following their release from the Cct/chaperonin complex, α- and β-tubulins interact with additional chaperone proteins that facilitate folding and heterodimer formation (Lopez-Fanarraga *et al.* 2001). These chaperones are collectively referred to as the TFCs and a schematic depicting this folding pathway is shown in Fig. 4a (Lewis *et al.* 1997; Szymanski 2002). This pathway has two separate arms involving chaperones specific for the α- and β-tubulins. The formation of the heterodimer is then mediated by a pair of shared cofactors that together help form the functional α/β heterodimer. Here, we found that P-bodies were present in log phase cultures of mutants lacking any of these TFC activities (Fig. 4b). Although there was substantial induction in all these mutants, the fraction of cells containing foci was highest for those strains defective for the two α-specific TFCs, Alf1 and Pac2. We also assessed P-body formation in *pat1*Δ

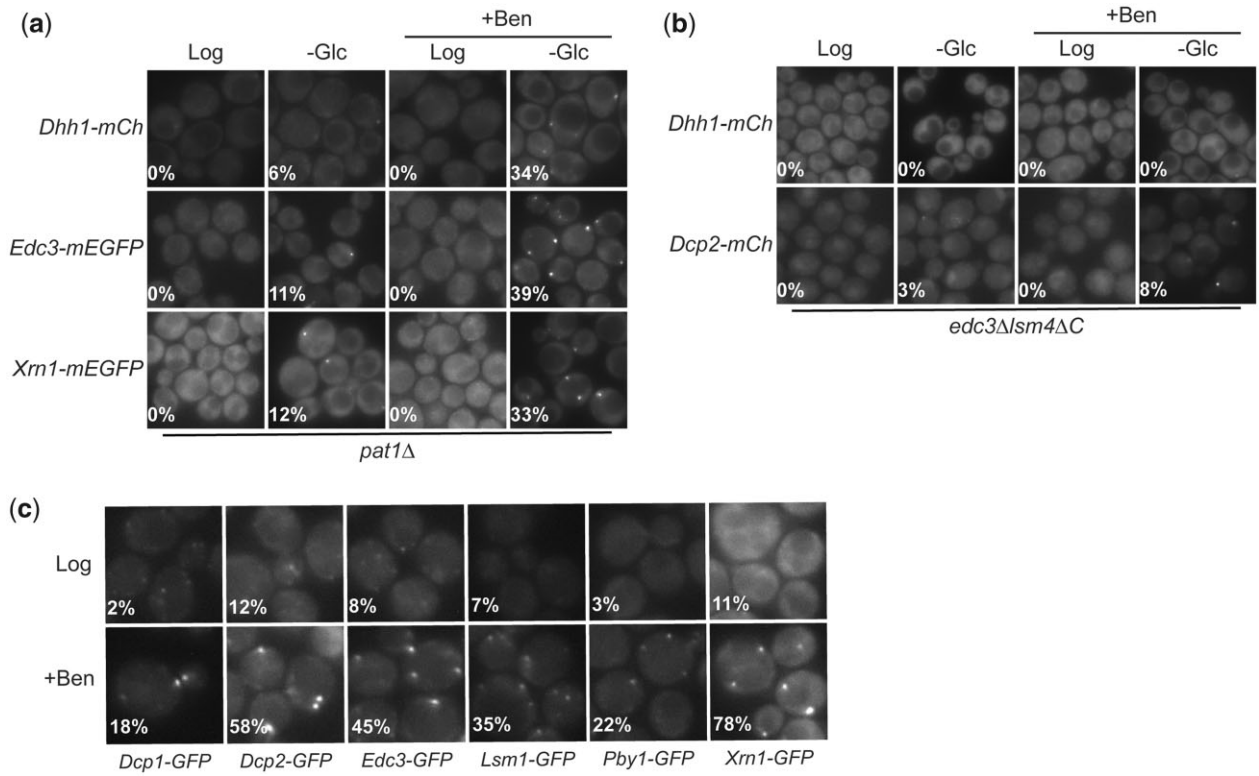

Fig. 3. Benomyl-mediated disruption of the microtubule network suppressed the *pat1*Δ P-body assembly defect. a, b) The effects of the microtubule depolymerizing drug, benomyl, on P-body assembly in the *pat1*Δ and *edc3*Δ *lsm4*ΔC mutants. Cells expressing the indicated P-body reporters were grown to mid-log phase (Log) and then transferred to a medium lacking glucose for 30 min (−Glc). Benomyl was added to a final concentration of 50 μg/ml to cells in each of these conditions, mid-log and glucose starved, and fluorescence microscopy was performed after a 60-min incubation. The fraction of cells containing a P-body-like focus is indicated for each condition. Data are shown for the *pat1*Δ strain in (a) and *edc3*Δ *lsm4*ΔC in (b). Note that benomyl specifically suppressed the P-body defect in the *pat1*Δ mutant. Scale bar, 5 μm. c) Benomyl treatment induced P-body-like foci in wild-type cells. Wild-type cells expressing the indicated P-body reporters were grown to mid-log phase and then treated with benomyl (15 μg/ml) for 60 min. Fluorescence microscopy was performed both before (Log) and after the benomyl treatment (+Ben). The fraction of cells containing a P-body-like focus is indicated. The observed differences in foci formation were determined to be statistically significant with a two-proportion Z-test where the resultant P-values were all less than 8×10^{-9}. The P-values for all relevant comparisons are provided in Supplementary Table 3.

cells and found that this defect was partially suppressed by the loss of most TFC activities (Fig. 4c). However, this suppression was typically more modest than that observed with the *pfd*Δ mutations but was again the strongest with the *pac2*Δ mutant. Thus, these data provided additional support for a model positing that the disruption of microtubule-related activities was responsible for the foci induction observed here. All of the conditions or mutations that resulted in foci formation are known to have an influence on tubulin monomer folding and/or the integrity of the cellular microtubule network.

The BIGs were morphologically distinct from P-bodies but still exhibited hallmarks of a liquid phase compartment

In *S. cerevisiae*, an exposure to stresses like glucose deprivation typically results in the formation of one, or perhaps two, large, bright P-body foci per cell (Fig. 5a). These granules tend to persist for as long as the inducing condition is imposed (Teixeira and Parker 2007; Shah *et al.* 2013). Here, we examined the granules that form in response to benomyl and found that they were morphologically distinct from these previous P-body examples. Following a treatment with benomyl, wild-type cells were found to have multiple (2–6) smaller foci of a more moderate intensity (Fig. 5a; see *Materials and Methods* for imaging details). To assess the persistence of these foci, a time-course was performed with cells expressing either a Dcp2- or Edc3-GFP reporter. The cells were treated with 50 μg/ml benomyl and followed by fluorescence microscopy for up to 3 h. In both cases, benomyl-induced foci were observed to form within 15 min and to persist throughout the 3-h incubation period (Fig. 5, b and c). However, although the Edc3 numbers remained relatively constant throughout the incubation period, there was a drop and subsequent rise in the number of cells containing Dcp2 foci following the 90-min timepoint. The significance of these Dcp2 fluctuations is not yet clear.

Despite these differences, both types of granules were found to exhibit characteristics of liquid-like condensates. For example, both were observed to be spherical, a shape that is associated with liquid structures so as to reduce surface tension (Fig. 5a) (Hyman *et al.* 2014). A second hallmark of these types of condensates is that they are sensitive to the aliphatic alcohol, 1,6-hexanediol. This reagent has been shown to disrupt condensates formed in both in vivo and in vitro settings (Kroschwald *et al.* 2017; Alberti *et al.* 2019). For example, P-bodies have been found to rapidly disperse when cells are treated with 1,6-hexanediol (Fig. 6a) (Kroschwald *et al.* 2017). We found that the benomyl-induced foci described here were similarly sensitive to this alcohol (Fig. 6a). For these studies, cells were exposed to benomyl to induce the P-body-like foci and 1,6-hexanediol was then added to a final concentration of 10% (v/v). The foci present were found to dissipate within 10 min at 30°C. A similar sensitivity to 1,6-hexanediol was also observed for the Dcp2-containing foci detected in *pfd1*Δ and *pac2*Δ cells (Fig. 6b). This sensitivity to 1,6-hexanediol

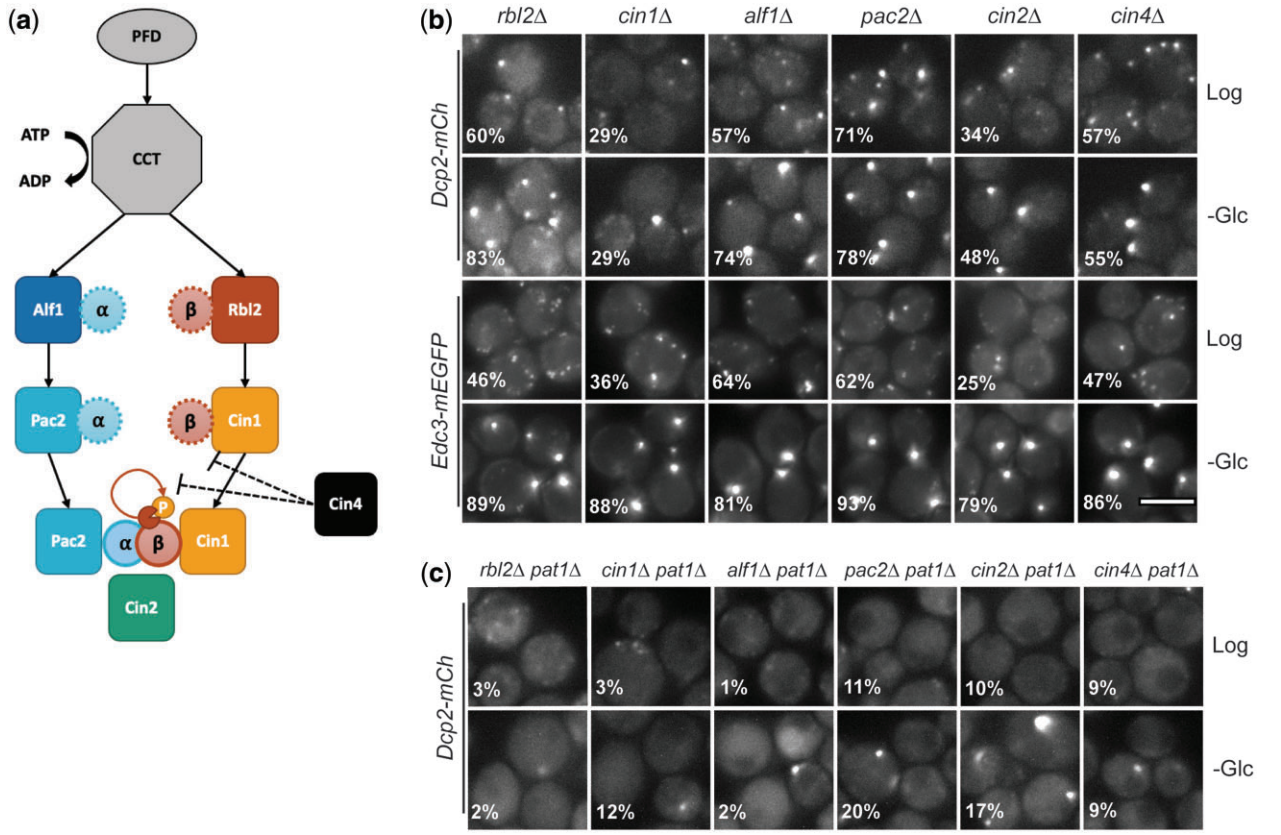

Fig. 4. Loss of TFC activity causes constitutive induction of P-body-like foci. a) A schematic depicting the folding pathway for tubulin monomers. Newly synthesized α/β-tubulin is bound by the prefoldin complex and escorted to Cct/chaperonin for ATP-dependent folding. Following release from the Cct/chaperonin complex, α/β-tubulin folding is mediated by isoform-specific folding cofactors. Subsequently, a Pac2–Cin2–Cin1 complex is formed which facilitates folding of a functional tubulin heterodimer. It has been proposed that Cin4 (analogous to human ARL2) may further participate in tubulin folding either through inhibiting the GAP-activity and/or preventing Cin1 interactions with β-tubulin (Bhamidipati *et al.* 2000). b) Mutants lacking TFC activities exhibited constitutive formation of P-body-like foci. *tfc*Δ mutants expressing the indicated P-body reporters were analyzed by fluorescence microscopy in the mid-log phase of growth (Log) and after 30 min of glucose deprivation (−Glc). The fraction of cells with a visible focus is indicated. The images shown are maximum intensity Z-projections (see *Materials and Methods* for more details). Scale bar, 5 μm. c) The loss of TFC activities suppressed the P-body assembly defect associated with the *pat1*Δ mutant. *tfc*Δ *pat1*Δ double mutants were analyzed by fluorescence microscopy as described in (b). The observed differences in foci formation were determined to be statistically significant with a two-proportion Z-test where the resultant *P*-values were all less than 5×10^{-8} (for b) or 4×10^{-2} (c). The *P*-values for all relevant comparisons are provided in Supplementary Table 3.

suggests that the granules described here are not irreversible aggregates of the tagged reporter proteins.

Finally, we asked whether the different P-body reporters examined here were located within the same foci following an exposure to benomyl. For this analysis, the degree of colocalization between Edc3, Dcp2, and Xrn1 was assessed in cells that had been either treated with benomyl or deprived of glucose. In both instances, we found that the level of colocalization between these reporters was greater than 85% (Fig. 6, c and d and Supplementary Fig. 4, a and b). These data therefore indicated that these P-body proteins were found within the same granules in benomyl-treated cells.

Several known P-body constituents were absent from the BIGs

To further define the foci induced by benomyl, we tested whether known P-body constituents were all present in these granules. Although most were associated with these structures (Fig. 3c), there were three notable exceptions, Pat1, Hrr25 and Dhh1. As indicated above, Pat1 is a conserved core constituent of P-body granules. However, we found that Pat1 was not associated to a significant degree with the foci that were induced by benomyl in wild-type cells after 15 or 30 min (Fig. 7a). There were some foci detected after 60 min, but these were typically much less intense than what was observed with other reporters, like Edc3 (see Fig. 5a). Pat1 was also absent from the cytoplasmic foci that were detected in the *pfd1*Δ, *pac2*Δ and *cct*^{ts} mutants (Figs. 2d and 7a). These latter mutants are all known to have defects in tubulin monomer folding (Lewis *et al.* 1997; Lopez-Fanarraga *et al.* 2001; Grantham *et al.* 2006; Gestaut *et al.* 2019). This lack of association with the benomyl-induced foci was interesting as these structures still appeared to require Pat1 for their formation. For example, *pat1*Δ cells formed significantly fewer foci in response to a benomyl treatment than the wild-type control (Fig. 3a). Thus, the Pat1 protein appears to have a role in the formation of BIGs, even though it is not a stable resident of these structures.

The second protein absent from BIGs was Hrr25, the yeast ortholog of the δ/ε isoform of the mammalian CK1 protein kinase (Fig. 7a) (DeMaggio *et al.* 1992; Fish *et al.* 1995). Hrr25 has been shown to be a constituent of the P-bodies induced by all conditions tested previously (Shah *et al.* 2013; Zhang *et al.* 2016). This association with the P-body protects Hrr25 from degradation by the proteasome and is essential for the normal completion of meiosis (Zhang *et al.* 2016, 2018). However, we found that Hrr25 was not associated with the foci induced by benomyl in wild-type cells nor with those detected in log phase cultures of the *pfd1*Δ

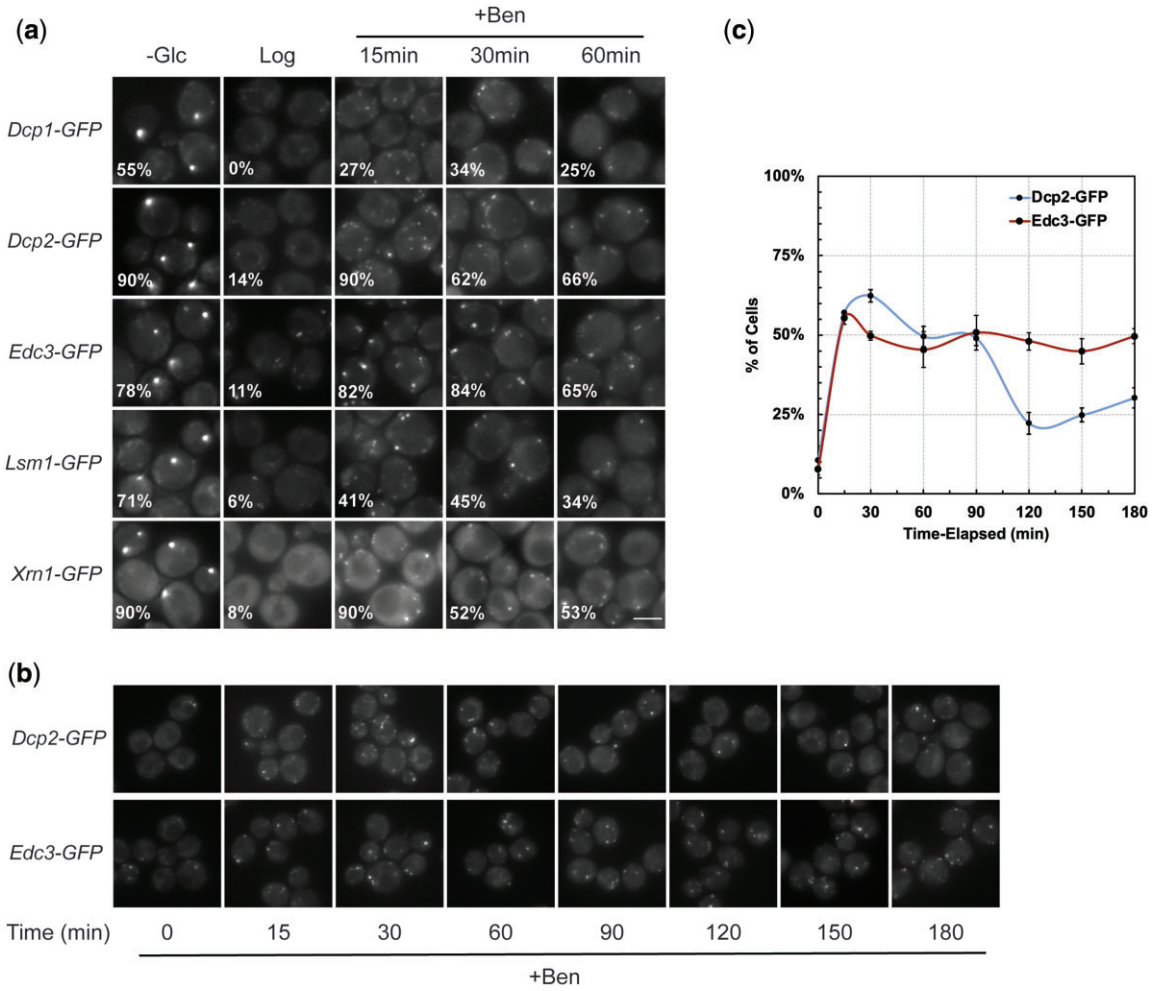

Fig. 5. The morphology and persistence of the BIGs. a) The foci induced by benomyl were morphologically distinct from P-bodies forming in response to glucose deprivation. Wild-type cells expressing the indicated P-body reporters were analyzed by fluorescence microscopy after 0, 15, 30, and 60 min of treatment with benomyl (50 μg/ml). The foci forming in response to glucose deprivation (30 min) are shown for comparison purposes. The images presented are maximum intensity Z-projections. The P-body reporters examined were Dcp1, Dcp2, Edc3, Lsm1, and Xrn1. Scale bar, 5 μm. b, c) A time-course of foci induction with benomyl. Wild-type cells expressing the indicated P-body reporters were incubated with benomyl (50 μg/ml) for the times shown and then examined by fluorescence microscopy. A graph showing the quantification of the data collected is presented in (c). For this experiment, the fraction of cells containing foci was evaluated with an intensity thresholding method described in the *Materials and Methods*. The observed differences in foci formation were determined to be statistically significant with a two-proportion Z-test where the resultant *P*-values were all less than 2×10^{-13}. The *P*-values for all relevant comparisons are provided in Supplementary Table 3.

and *pac2*Δ mutants (Fig. 7a). In contrast, this protein kinase was detected within the foci that form in cells that were subjected concurrently to both a benomyl treatment and glucose deprivation (Fig. 7, b and c). This latter association was observed in wild-type and *pat1*Δ cells. In both strains, these latter Hrr25 foci were also found to contain the P-body constituents, Dcp2 and Edc3; the colocalization observed was found to approach 100% in all instances (Fig. 7, b and c). These results suggested that the presence of Hrr25 in P-body-like foci may be regulated by glucose availability. However, the key point here is that Hrr25 was not present within the P-body-like granules that were induced by conditions, like benomyl, that disrupt microtubule integrity and/or function.

The third protein of note is another conserved constituent of P-body granules, the RNA helicase, Dhh1 (Coller *et al.* 2001; Cheng *et al.* 2005; Xing *et al.* 2020). In this case, the association with BIGs was found to be dependent upon the benomyl concentration used. Although Dhh1 was not associated with the foci induced by 15 μg/ml benomyl, it was detected within the granules produced in response to higher concentrations of this drug, like 50 μg/ml (Fig. 7a and Supplementary Fig. 5). However, in this latter case, the recruitment to foci was significantly delayed relative to that of other reporters, like Dcp2 and Edc3 (Figs. 5a and 7a). This delay in recruitment for Dhh1 has not been observed for the P-bodies induced by glucose deprivation. Notably, Dhh1 was also absent from the foci that were constitutively present in the *pfd1*Δ and *pac2*Δ strains (Fig. 7a). In all, these data indicated that there were compositional differences between the benomyl-induced foci observed here and the more traditional P-bodies described previously.

The α-tubulin, Tub3, was not associated with the benomyl-induced foci

We also asked whether α-tubulin was associated with the BIGs described here. This possibility was suggested by previous work that found a Tub1-GFP fusion protein in the P-body-like foci induced by benomyl (Sweet *et al.* 2007). *S. cerevisiae* has two α-tubulins, a major isoform, Tub1, and a more minor form, Tub3

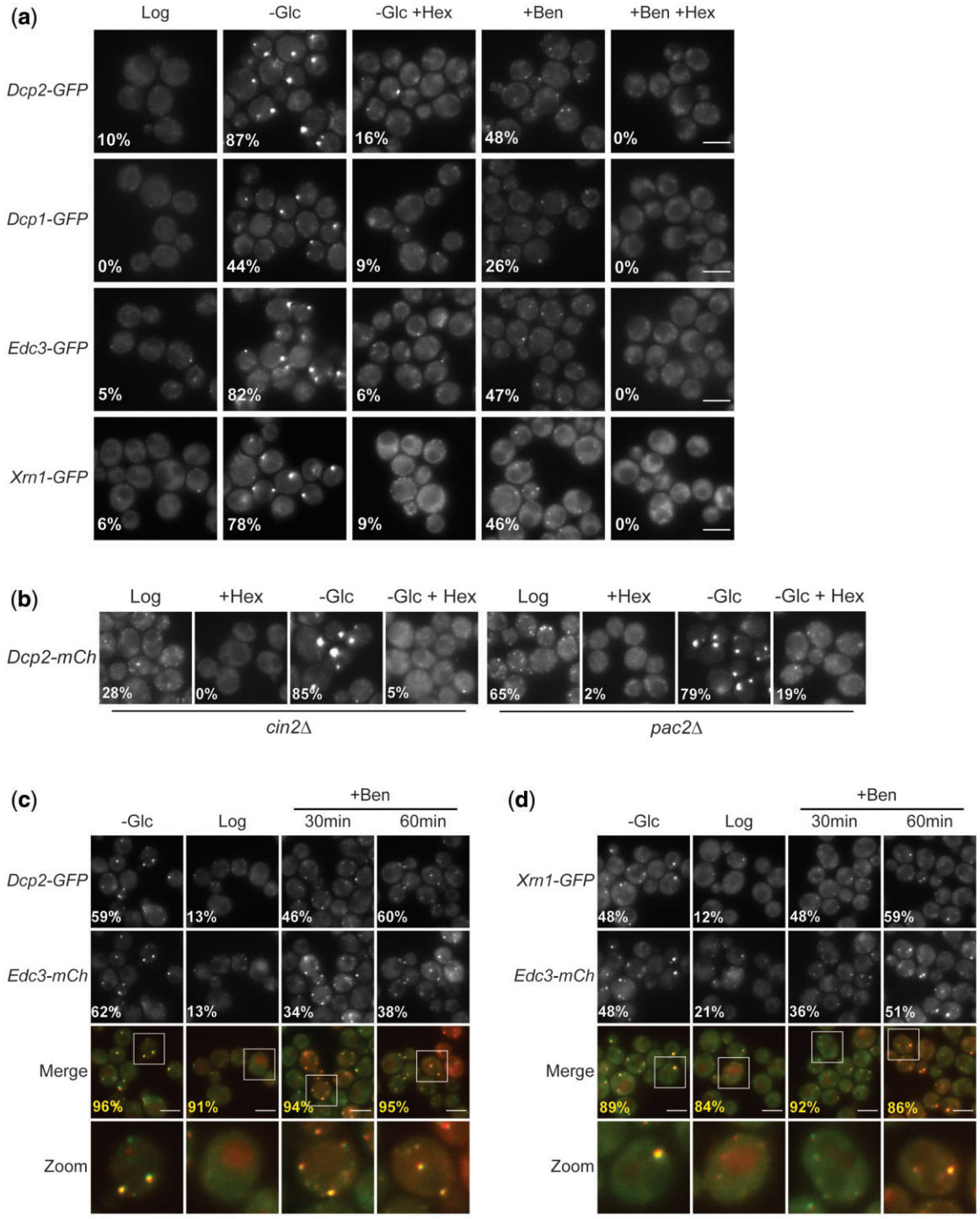

Fig. 6. The P-body-like foci induced by microtubule perturbations contain multiple P-body reporters and exhibit hallmarks of liquid-like condensates. a) BIGs are dispersed by treatment with the aliphatic alcohol, 1,6-hexanediol. Wild-type cells containing granules induced by either glucose deprivation or a benomyl treatment were incubated with 1,6-hexanediol (10% v/v) for 10 min and then examined by fluorescence microscopy. The granules were marked by the GFP-tagged reporters, Dcp1, Dcp2, Edc3, and Xrn1. The fraction of cells with a visible focus is indicated. Scale bar, 5 μm. b) The constitutive P-body-like foci in the *tfc*Δ mutants, *cin2*Δ and *pac2*Δ, were also sensitive to 1,6-hexanediol treatment. The granules present in either mid-log phase (Log) or glucose-deprived (−Glc) cells were visualized by fluorescence microscopy both before and after the cells were treated with 1,6-hexanediol. The fraction of cells with a visible Dcp2-mCh focus is indicated. c, d) The BIGs contain multiple P-body reporters. The colocalization between the P-body reporters, Dcp2, Edc3, and Xrn1, was assessed for the granules induced by either glucose deprivation (−Glc) or benomyl treatment. Colocalization was evaluated by fluorescent microscopy. The fraction of cells containing a focus for each P-body reporter (white) and the percentage of colocalization between the P-body reporters (yellow, Merge) are indicated. The % colocalization was calculated as described in the *Materials and Methods*. The bottom row shows an enlarged view of the indicated cells for each condition. Scale bar, 5 μm. The observed differences in foci presence were determined to be statistically significant with a two-proportion Z-test where the resultant P-values were all less than 2.2×10^{-16}. The P-values for all relevant comparisons are provided in Supplementary Table 3.

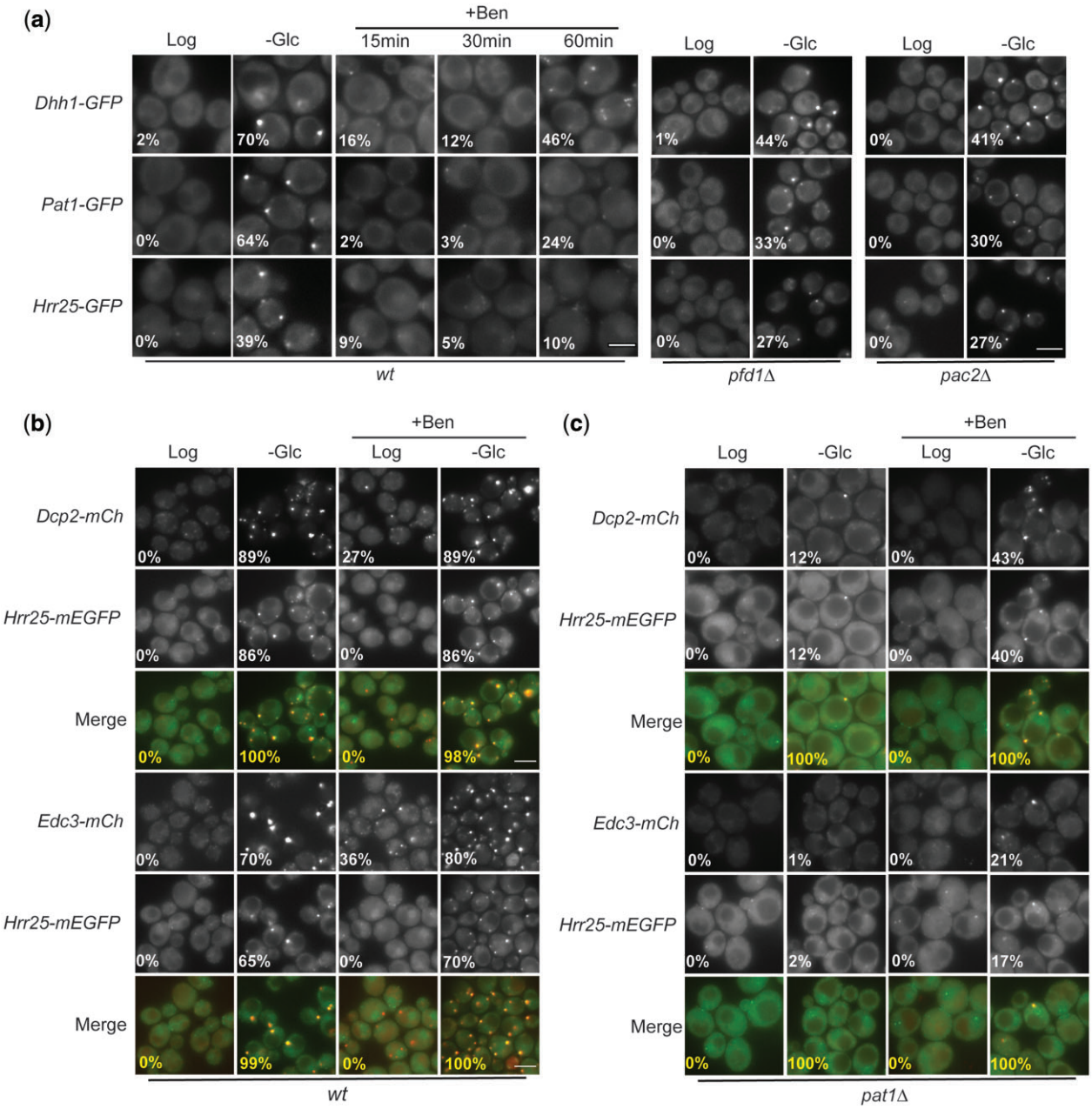

Fig. 7. Key P-body constituents were absent from the granules induced by disruption of the microtubule network. a) The differential localization of Dhh1, Hrr25, and Pat1 in P-bodies and BIGs. Wild-type cells (*wt*) expressing the Dhh1-, Hrr25-, and Pat1-GFP reporters were examined by fluorescence microscopy during log phase growth (Log), after glucose deprivation (−Glc) or following treatment with benomyl (50 μg/ml) for the indicated times. Log phase and glucose-deprived cultures of the *pfd1*Δ and *pac2*Δ mutants expressing these same P-body reporters were also analyzed by fluorescence microscopy. The fraction of cells containing a focus is indicated for each condition. Scale bar, 5 μm. b, c) Hrr25 was not localized to the granules induced by benomyl treatment alone. The colocalization of Hrr25-mEGFP with either Dcp2- or Edc3-mCh was assessed by fluorescence microscopy in wild-type (*wt*) and *pat1*Δ cells under the indicated conditions. The cells were examined during log phase growth (Log), after a 60-min benomyl treatment (Log, +Ben), after a 60-min period of glucose deprivation (−Glc) and after both glucose deprivation and benomyl treatment (−Glc, +Ben). The fraction of cells containing a focus for each P-body reporter and the percentage of colocalization between the P-body reporters (Merge) are indicated. The % colocalization was calculated as described in the *Materials and Methods*. Note that Hrr25 as only recruited to granules in those cells that had been deprived of glucose. Scale bar, 5 μm.

(Richards *et al.* 2000). The Tub1 fusion used in this prior study was obtained from a commercially available collection of strains that express GFP fusion proteins. However, our sequence analysis indicated that this Tub1-GFP construct was not correct and that this strain was instead expressing an unnatural variant of Tub3. Specifically, this strain expressed a Tub3 protein that had 2 additional glutamic acid residues inserted before the terminal phenylalanine (Supplementary Fig. 6a; see *Materials and Methods* for more details). Thus, to test whether an α-tubulin was present in the foci observed here, we used strains expressing a Tub3-GFP reporter that was verified by a sequence analysis (Supplementary Fig. 6a). For these studies, we assessed the colocalization between Tub3 and 3 P-body reporters, Dcp2, Edc3, and Xrn1, in cells that had been treated with 50 μg/ml benomyl. In all cases, we found no significant colocalization between Tub3 and the P-body reporter (Fig. 8, a–c). We also found no colocalization between Tub3

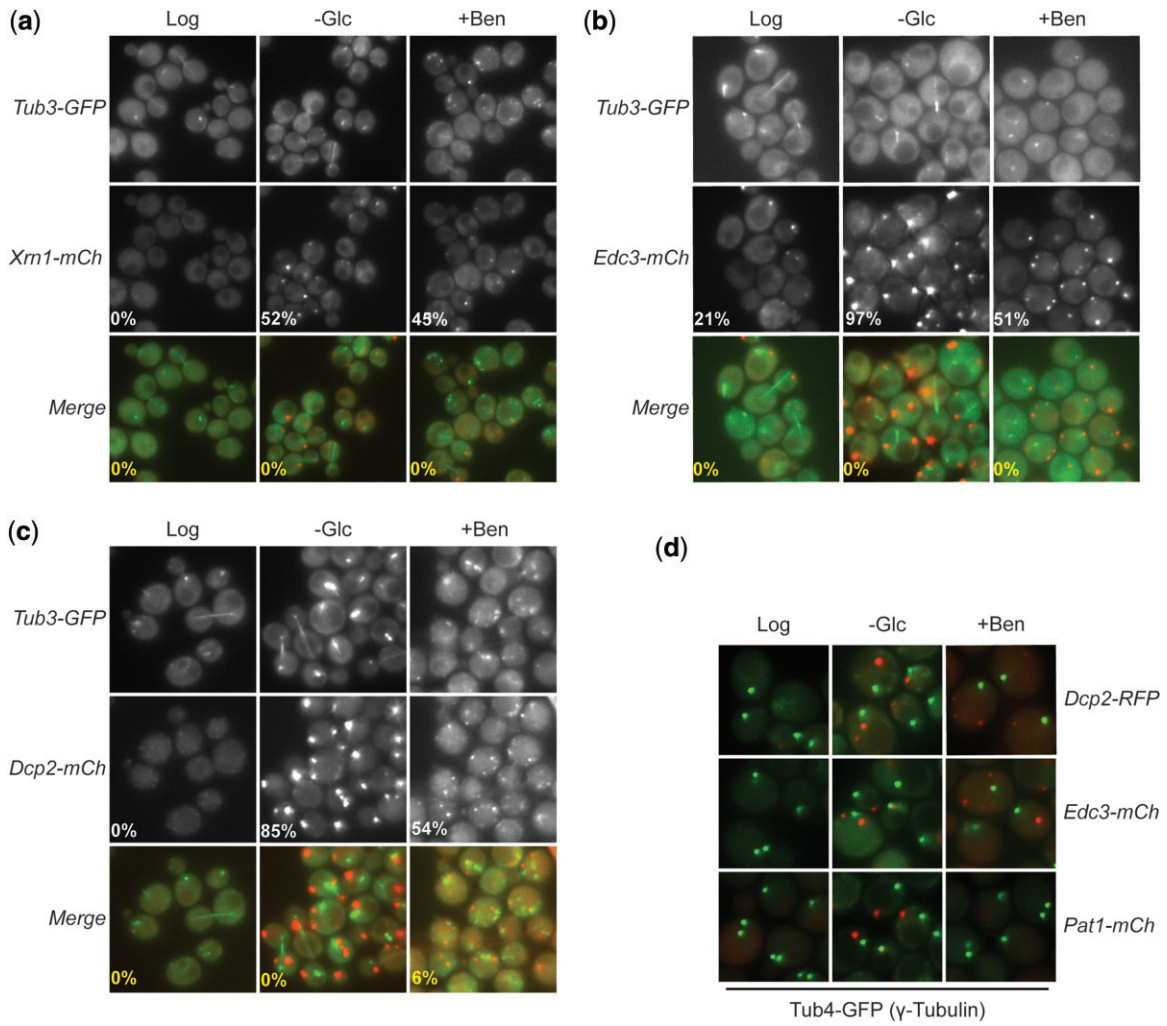

Fig. 8. The P-body-like granules induced by benomyl did not contain the α-tubulin isoform, Tub3. a–c) Wild-type cells expressing Tub3-GFP and the indicated mCh-tagged P-body reporters were examined by fluorescence microscopy during log phase growth (Log), after a period of glucose deprivation (−Glc) and following a 60-min treatment with 50 μg/ml benomyl (+Ben). The fraction of cells containing a focus for each P-body reporter (white) and percentage of colocalization between Tub3 and the different P-body reporters (yellow) are indicated. The % colocalization between Tub3 and each P-body reporter was assessed as described in the *Materials and Methods*. d) The Tub4 γ-tubulin was not localized to the P-body-like granules induced by either benomyl or a glucose deprivation. Wild-type cells expressing Tub4-GFP and the indicated P-body reporters were examined by fluorescence microscopy under the same conditions as described for (a)–(c).

and these reporters in cells that had been deprived of glucose so as to trigger the induction of traditional P-body granules (Fig. 8, a–c). Dcp2 also failed to colocalize with a GFP-tagged version of Tub4, the γ-tubulin analog in *S. cerevisiae* (Fig. 8d). Consistent with the microscopy data, we found that the α-tubulin proteins were not present in Dcp2 immunoprecipitates isolated from cells that had been treated with benomyl (Supplementary Fig. 6b). Thus, we found no evidence for the presence of α-tubulin in either the BIGs described here or the more traditional P-body foci that form in response to glucose deprivation.

The benomyl-induced foci were not regulated by the PKA signaling pathway

Given the above differences, we were interested in whether the assembly of BIGs might be regulated differently than traditional P-bodies. Of particular interest was the role played by the PKA signaling pathway. PKA has been shown to inhibit P-body formation in *S. cerevisiae* via the direct phosphorylation of Pat1 (Ramachandran *et al.* 2011). A reduction in PKA activity is thus generally required for efficient P-body assembly. For example, PKA activity diminishes rapidly upon glucose deprivation and this decrease is necessary for the ensuing induction of P-body foci (Ramachandran *et al.* 2011; Shah *et al.* 2013). Here, we tested whether PKA levels were affected by the presence of benomyl. For this analysis, we used a PKA biosensor that contains an N-terminal fragment of the choline kinase, Cki1 (Fig. 9a) (Deminoff *et al.* 2006). This fragment has two documented PKA sites, and when phosphorylated this reporter migrates more slowly in SDS-polyacrylamide gels. The ratio of the phosphorylated and non-phosphorylated forms of the reporter serves as a relative measure of the in vivo levels of PKA activity (Deminoff *et al.* 2006; Ramachandran and Herman 2011). We examined this biosensor by western blotting with extracts prepared from wild-type cells both before and after a benomyl treatment. This analysis indicated that neither the total level nor the ratio of the two forms of this biosensor were significantly affected by the presence of this

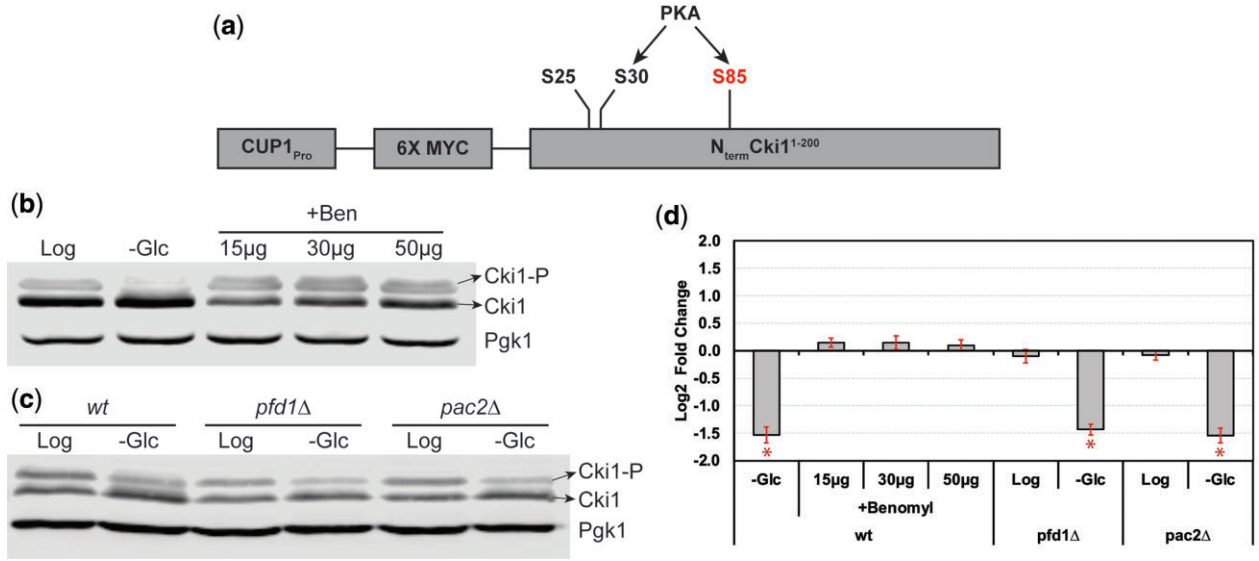

Fig. 9. PKA signaling activity was not affected by benomyl treatment or in cells lacking prefoldin or TFC activities. a) A schematic of the Cki1 reporter used for these studies is shown indicating the two sites of PKA phosphorylation, Ser30 and Ser85 (Deminoff *et al.* 2006). b) PKA activity in wild-type cells was not affected by the presence of benomyl. Protein extracts were prepared from wild-type cells expressing this Cki1 reporter during log phase growth (Log), after glucose deprivation (−Glc) or following treatment with the indicated concentrations of benomyl (per ml) for 60 min. Western blots were performed with an anti-Myc epitope antibody to assess the relative levels of the phosphorylated (Cki1-P) and nonphosphorylated (Cki1) forms of this reporter under each condition. Pgk1 was used as a loading control for this experiment. c) PKA activity was not altered in mutants defective for prefoldin (*pfd1*Δ) or TFC (*pac2*Δ) activities. Protein extracts were prepared from wild-type, *pfd1*Δ and *pac2*Δ cells expressing this Cki1 reporter during log phase growth (Log) and after glucose deprivation (−Glc). Western blots were then performed as described above in (b). d) Quantification of the data presented in (b) and (c). The graph indicates the $\log_2$ fold change of the Cki1-P to Cki1 ratio for the indicated strains and treatment conditions. As previously reported, glucose deprivation resulted in a significant reduction of PKA activity. The asterisks indicate those values that vary from the wild-type log phase control in a statistically significant manner with *P*-values determined by a paired *t*-test to be less than 3.2×10^{-2}.

drug (Fig. 9, b and d). In contrast, the level of the phosphorylated form of this biosensor decreased dramatically upon glucose deprivation (Fig. 9, b–d). The relative levels of this biosensor were also unaffected in the *pfd1*Δ and *pac2*Δ mutant strains that had elevated levels of P-body-like foci (Fig. 9, c and d). Altogether, these results indicated that PKA signaling activity was not affected by the presence of benomyl and that the BIGs described here must be responding to some other regulatory signals.

Discussion

This study found that P-body-like granules form in response to conditions that disrupt microtubule integrity in the budding yeast, *S. cerevisiae*. The P-body is a cytoplasmic membraneless organelle that has been implicated in the decay and/or storage of mRNAs. The initial finding here was that the P-body assembly defect in *pat1*Δ mutants was suppressed by mutations that inactivate the prefoldin-Cct/chaperonin folding pathway. The Pat1 protein is a conserved constituent of P-bodies that is required for efficient granule formation (Teixeira and Parker 2007; Pilkington and Parker 2008). Subsequent work indicated that this suppression was likely due to a failure to properly fold tubulin monomers in these mutants. For example, similar P-body-like granules were detected in mutants defective for any of the tubulin-specific chaperones, known as the TFCs, and in wild-type cells that were treated with the drug, benomyl. Benomyl binds to β-tubulin and disrupts the integrity of microtubules in *S. cerevisiae* (Hochwagen *et al.* 2005; Vela-Corcía *et al.* 2018). The granules identified were found to contain known P-body markers and to exhibit traits consistent with condensates that form by liquid-liquid phase separation. In all, these data indicated that perturbations of the microtubule network trigger the induction of cytoplasmic granules that resemble the previously described P-body.

Further work indicated that these BIGs differ from traditional P-bodies in a number of interesting ways. The differences included aspects of protein composition, granule morphology, and the manner in which induction was regulated. With respect to the former, we found that several key P-body constituents were absent from BIGs. These included the aforementioned Pat1 and the CK1 protein kinase homolog, Hrr25. Both of these proteins have been found to be associated with the P-bodies induced by all conditions described to date. The Dhh1 RNA helicase was also either absent from BIGs or recruited to these foci only after an extended delay. The absence of Pat1 is particularly interesting as this protein was still required for the efficient formation of BIGs. Thus, Pat1 appears to have a role in granule formation, even though it is not a stable resident of this structure. Finally, the data here suggest that the formation of BIGs is not regulated by PKA signaling activity. P-body formation was shown previously to be inhibited by PKA via the direct phosphorylation of the Pat1 protein (Ramachandran *et al.* 2011; Shah *et al.* 2013). Thus, BIG induction must be regulated by some other means independent of this signaling pathway.

Altogether, these data suggest that BIGs exhibit features that distinguish them from the P-bodies that are induced by stress conditions like glucose deprivation. Although the significance of these differences is not yet clear, it is possible that BIGs represent a particular subtype of P-body with distinct physiological roles in cells. For example, previous work has implicated P-bodies in two competing aspects of mRNA metabolism, decay and storage (Eulalio *et al.* 2007; Balagopal and Parker 2009; Arribere *et al.* 2011; Zid and O'Shea 2014; Hubstenberger *et al.* 2017; Standart and Weil 2018). The BIGs described here could be associated with one

of these activities and the ultimate choice between the two could be controlled by the inclusion (or not) of specific P-body constituents in the granules. The presence of different functional classes of a membraneless organelle that are distinguished by protein composition is something that has been suggested previously (Mitrea and Kriwacki 2016; Boeynaems *et al.* 2018; Gomes and Shorter 2019; Zhang and Herman 2020). In this light, it will be interesting to determine whether any of the P-body-like granules identified recently might differ in similar ways from those induced by stresses like glucose deprivation (Loll-Krippleber and Brown 2017; García *et al.* 2019). Additional work is clearly needed to test these types of possibilities and to ultimately determine the physiological role of BIGs in eukaryotic cells.

The final point here concerns the relationship between BIGs and microtubules. More precisely, how does the disruption of microtubule integrity and/or function trigger the formation of these granules? A possibility that was suggested previously is that P-body proteins could be associated with microtubules and that this association would restrict protein movement (Sweet *et al.* 2007; Aizer *et al.* 2008). The disruption of the microtubule network would then free up these proteins and allow them to assemble into the observed granules. However, there is little evidence to date of any such association between P-body proteins and microtubule polymers. Alternatively, the release of tubulin monomers (or dimers) could be responsible for the stimulation of granule formation. Although we did not detect any α-tubulin association with BIGs, these effects could be indirect or involve microtubule-associated components other than the tubulin monomers themselves. Another intriguing possibility is that the formation of these granules could occur as a consequence of a tubulin-related regulatory phenomenon like the autoregulation that has been described in animal cells (Gay *et al.* 1987; Katz *et al.* 1990; Gasic and Mitchison 2019). In this process, tubulin mRNAs are targeted for degradation by an unknown mechanism when microtubule integrity is breached (Gasic and Mitchison 2019). However, it should be noted that there is no evidence for this regulatory paradigm in *S. cerevisiae* and several studies have suggested that this process does not occur in this budding yeast (Katz *et al.* 1990; Weinstein and Solomon 1990; Theodorakis 1994). In any case, it will be important to understand why P-body-like granules form in response to microtubule disruption and to determine whether these granules have any role in the regulation of microtubule dynamics.

Data availability

All strains and plasmids are available upon request. The authors affirm that all data necessary for confirming the conclusions of the article are present within the article, figures, and tables.

Supplemental material is available at *GENETICS* online.

Acknowledgments

We thank Drs. Jeff Coller, Anita Hopper, and Jeremy Thorner for reagents used in this study, the Genomics Shared Resource at OSU for DNA sequencing (supported in part by National Cancer Institute grant P30 CA016058), Dr. Greg Booton for assistance with the statistical analyses, and members of the Herman lab, especially Priscila Rodriguez Garcia, for helpful discussions and comments on the article.

Funding

This work was supported by National Institutes of Health grant R01 GM128440 to PKH.

Conflicts of interest

None declared.

Literature cited

Aizer A, Brody Y, Ler LW, Sonenberg N, Singer RH, Shav-Tal Y. The dynamics of mammalian P body transport, assembly, and disassembly in vivo. Mol Biol Cell. 2008;19(10):4154–4166.

Alberti S. Phase separation in biology. Curr Biol. 2017;27(20): R1097–R1102.

Alberti S, Gladfelter A, Mittag T. Considerations and challenges in studying liquid-liquid phase separation and biomolecular condensates. Cell. 2019;176(3):419–434.

Anderson P, Kedersha N. RNA granules: post-transcriptional and epigenetic modulators of gene expression. Nat Rev Mol Cell Biol. 2009;10(6):430–436.

Arribere JA, Doudna JA, Gilbert WV. Reconsidering movement of eukaryotic mRNAs between polysomes and P bodies. Mol Cell. 2011; 44(5):745–758.

Balagopal V, Parker R. Polysomes, P bodies and stress granules: states and fates of eukaryotic mRNAs. Curr Opin Cell Biol. 2009; 21(3):403–408.

Banani SF, Lee HO, Hyman AA, Rosen MK. Biomolecular condensates: organizers of cellular biochemistry. Nat Rev Mol Cell Biol. 2017;18(5):285–298.

Bashkirov VI, Scherthan H, Solinger JA, Buerstedde JM, Heyer WD. A mouse cytoplasmic exoribonuclease (mXRN1p) with preference for G4 tetraplex substrates. J Cell Biol. 1997;136(4):761–773.

Beggs JD. Lsm proteins and RNA processing. Biochem Soc Trans. 2005;33(Pt 3):433–438.

Bhamidipati A, Lewis SA, Cowan NJ. ADP ribosylation factor-like protein 2 (Arl2) regulates the interaction of tubulin-folding cofactor D with native tubulin. J Cell Biol. 2000;149(5):1087–1096.

Boehning M, Dugast-Darzacq C, Rankovic M, Hansen AS, Yu T, Marie-Nelly H, McSwiggen DT, Kokic G, Dailey GM, Cramer P, *et al.* RNA polymerase II clustering through carboxy-terminal domain phase separation. Nat Struct Mol Biol. 2018;25(9):833–840.

Boeynaems S, Alberti S, Fawzi NL, Mittag T, Polymenidou M, Rousseau F, Schymkowitz J, Shorter J, Wolozin B, Van Den Bosch L, *et al.* Protein phase separation: a new phase in cell biology. Trends Cell Biol. 2018;28(6):420–435.

Boisvert FM, van Koningsbruggen S, Navascues J, Lamond AI. The multifunctional nucleolus. Nat Rev Mol Cell Biol. 2007;8(7): 574–585.

Bolte S, Cordelières FP. A guided tour into subcellular colocalization analysis in light microscopy. J Microsc. 2006;224(Pt 3):213–232.

Bouveret E, Rigaut G, Shevchenko A, Wilm M, Seraphin B. A Sm-like protein complex that participates in mRNA degradation. EMBO J. 2000;19(7):1661–1671.

Brangwynne CP, Mitchison TJ, Hyman AA. Active liquid-like behavior of nucleoli determines their size and shape in *Xenopus laevis* oocytes. Proc Natl Acad Sci U S A. 2011;108(11):4334–4339.

Braun JE, Tritschler F, Haas G, Igreja C, Truffault V, Weichenrieder O, Izaurralde E. The C-terminal alpha-alpha superhelix of Pat is required for mRNA decapping in metazoa. EMBO J. 2010;29(14): 2368–2380.

Budovskaya YV, Hama H, DeWald DB, Herman PK. The C terminus of the Vps34p phosphoinositide 3-kinase is necessary and sufficient for the interaction with the Vps15p protein kinase. J Biol Chem. 2002;277(1):287–294.

Cheng Z, Coller J, Parker R, Song H. Crystal structure and functional analysis of DEAD-box protein Dhh1p. RNA. 2005;11(8):1258–1270.

Coller J, Parker R. General translational repression by activators of mRNA decapping. Cell. 2005;122(6):875–886.

Coller JM, Tucker M, Sheth U, Valencia-Sanchez MA, Parker R. The DEAD box helicase, Dhh1p, functions in mRNA decapping and interacts with both the decapping and deadenylase complexes. RNA. 2001;7(12):1717–1727.

Cougot N, Babajko S, Seraphin B. Cytoplasmic foci are sites of mRNA decay in human cells. J Cell Biol. 2004;165(1):31–40.

Cox KH, Tate JJ, Cooper TG. Actin cytoskeleton is required for nuclear accumulation of Gln3 in response to nitrogen limitation but not rapamycin treatment in *Saccharomyces cerevisiae*. J Biol Chem. 2004;279(18):19294–19301.

DeCaprio J, Kohl TO. Lysing yeast cells with glass beads for immunoprecipitation. Cold Spring Harbor Protoc. 2020;2020(11): pdb.prot098590.

Decker CJ, Teixeira D, Parker R. Edc3p and a glutamine/asparagine-rich domain of Lsm4p function in processing body assembly in *Saccharomyces cerevisiae*. J Cell Biol. 2007;179(3):437–449.

DeMaggio AJ, Lindberg RA, Hunter T, Hoekstra MF. The budding yeast HRR25 gene product is a casein kinase I isoform. Proc Natl Acad Sci U S A. 1992;89(15):7008–7012.

Deminoff SJ, Howard SC, Hester A, Warner S, Herman PK. Using substrate-binding variants of the cAMP-dependent protein kinase to identify novel targets and a kinase domain important for substrate interactions in *Saccharomyces cerevisiae*. Genetics. 2006; 173(4):1909–1917.

Deminoff SJ, Ramachandran V, Herman PK. Distal recognition sites in substrates are required for efficient phosphorylation by the cAMP-dependent protein kinase. Genetics. 2009;182(2):529–539.

Eulalio A, Behm-Ansmant I, Izaurralde E. P bodies: at the crossroads of post-transcriptional pathways. Nat Rev Mol Cell Biol. 2007;8(1): 9–22.

Eystathioy T, Jakymiw A, Chan EKL, Séraphin B, Cougot N, Fritzler MJ. The GW182 protein colocalizes with mRNA degradation associated proteins hDcp1 and hLSm4 in cytoplasmic GW bodies. RNA. 2003;9(10):1171–1173.

Fish KJ, Cegielska A, Getman ME, Landes GM, Virshup DM. Isolation and characterization of human casein kinase I epsilon (CKI), a novel member of the CKI gene family. J Biol Chem. 1995;270(25): 14875–14883.

Franks TM, Lykke-Andersen J. The control of mRNA decapping and P-body formation. Mol Cell. 2008;32(5):605–615.

García R, Pulido V, Orellana-Muñoz S, Nombela C, Vázquez de Aldana CR, Rodríguez-Peña JM, Arroyo J. Signalling through the yeast MAPK Cell Wall Integrity pathway controls P-body assembly upon cell wall stress. Sci Rep. 2019;9(1):13.

Gasic I, Mitchison TJ. Autoregulation and repair in microtubule homeostasis. Curr Opin Cell Biol. 2019;56:80–87.

Gay DA, Yen TJ, Lau JTY, Cleveland DW. Sequences that confer beta-tubulin autoregulation through modulated mRNA stability reside within exon 1 of a beta-tubulin mRNA. Cell. 1987; 50(5):671–679.

Geissler S, Siegers K, Schiebel E. A novel protein complex promoting formation of functional α- and γ-tubulin. EMBO J. 1998;17(4): 952–966.

Gestaut D, Roh SH, Ma B, Pintilie G, Joachimiak LA, Leitner A, Walzthoeni T, Aebersold R, Chiu W, Frydman J, *et al.* The chaperonin TRiC/CCT associates with prefoldin through a conserved electrostatic interface essential for cellular proteostasis. Cell. 2019;177(3):751–765. e715.

Gietz RD, Schiestl RH. High-efficiency yeast transformation using the LiAc/SS carrier DNA/PEG method. Nat Protoc. 2007;2(1): 31–34.

Gomes E, Shorter J. The molecular language of membraneless organelles. J Biol Chem. 2019;294(18):7115–7127.

Grantham J, Brackley KI, Willison KR. Substantial CCT activity is required for cell cycle progression and cytoskeletal organization in mammalian cells. Exp Cell Res. 2006;312(12):2309–2324.

Hartl FU, Bracher A, Hayer-Hartl M. Molecular chaperones in protein folding and proteostasis. Nature. 2011;475(7356):324–332.

Ho Y, Gruhler A, Heilbut A, Bader GD, Moore L, Adams S-L, Millar A, Taylor P, Bennett K, Boutilier K, *et al.* Systematic identification of protein complexes in *Saccharomyces cerevisiae* by mass spectrometry. Nature. 2002;415(6868):180–183.

Hochwagen A, Wrobel G, Cartron M, Demougin P, Niederhauser-Wiederkehr C, Boselli MG, Primig M, Amon A. Novel response to microtubule perturbation in meiosis. Mol Cell Biol. 2005;25(11): 4767–4781.

Hubstenberger A, Courel M, Bénard M, Souquere S, Ernoult-Lange M, Chouaib R, Yi Z, Morlot J-B, Munier A, Fradet M, *et al.* P-body purification reveals the condensation of repressed mRNA regulons. Mol Cell. 2017;68(1):144–157. e145.

Huch S, Müller M, Muppavarapu M, Gommlich J, Balagopal V, Nissan T. The decapping activator Edc3 and the Q/N-rich domain of Lsm4 function together to enhance mRNA stability and alter mRNA decay pathway dependence in *Saccharomyces cerevisiae*. Biol Open. 2016;5(10):1388–1399.

Huch S, Nissan T. An mRNA decapping mutant deficient in P body assembly limits mRNA stabilization in response to osmotic stress. Sci Rep. 2017;7:44395–44395.

Huh W-K, Falvo JV, Gerke LC, Carroll AS, Howson RW, Weissman JS, O'Shea EK. Global analysis of protein localization in budding yeast. Nature. 2003;425(6959):686–691.

Hyman AA, Weber CA, Julicher F. Liquid-liquid phase separation in biology. Annu Rev Cell Dev Biol. 2014;30:39–58.

Ingelfinger D, Arndt-Jovin DJ, Luhrmann R, Achsel T. The human LSm1-7 proteins colocalize with the mRNA-degrading enzymes Dcp1/2 and Xrnl in distinct cytoplasmic foci. RNA. 2002;8(12): 1489–1501.

Katz W, Weinstein B, Solomon F. Regulation of tubulin levels and microtubule assembly in *Saccharomyces cerevisiae*: consequences of altered tubulin gene copy number. Mol Cell Biol. 1990;10(10): 5286–5294.

Kozubowski L, Aboobakar EF, Cardenas ME, Heitman J. Calcineurin colocalizes with P-bodies and stress granules during thermal stress in *Cryptococcus neoformans*. Eukaryot Cell. 2011;10(11): 1396–1402.

Kroschwald S, Maharana S, Simon A. Hexanediol: a chemical probe to investigate the material properties of membrane-less compartments. Matters. 2017:1–6. Doi: 10.19185/matters.201702000010.

Kroschwald S, Munder MC, Maharana S, Franzmann TM, Richter D, Ruer M, Hyman AA, Alberti S. Different material states of Pub1 condensates define distinct modes of stress adaptation and recovery. Cell Rep. 2018;23(11):3327–3339.

Kshirsagar M, Parker R. Identification of Edc3p as an enhancer of mRNA decapping in *Saccharomyces cerevisiae*. Genetics. 2004; 166(2):729–739.

LeBlanc BM, Moreno RY, Escobar EE, Venkat Ramani MK, Brodbelt JS, Zhang Y. What's all the phos about? Insights into the

phosphorylation state of the RNA polymerase II C-terminal domain: via mass spectrometry. RSC Chem Biol. 2021;2(4): 1084–1095.
Lewis SA, Tian G, Cowan NJ. The α- and β-tubulin folding pathways. Trends Cell Biol. 1997;7(12):479–484.
Li P, Banjade S, Cheng H-C, Kim S, Chen B, Guo L, Llaguno M, Hollingsworth JV, King DS, Banani SF, *et al.* Phase transitions in the assembly of multivalent signalling proteins. Nature. 2012; 483(7389):336–340.
Li Q, Lau A, Morris TJ, Guo L, Fordyce CB, Stanley EF. A Syntaxin 1, Gαo, and N-type calcium channel complex at a presynaptic nerve terminal: analysis by quantitative immunocolocalization. J Neurosci. 2004;24(16):4070–4081.
Li Z, Vizeacoumar FJ, Bahr S, Li J, Warringer J, Vizeacoumar FS, Min R, Vandersluis B, Bellay J, Devit M, *et al.* Systematic exploration of essential yeast gene function with temperature-sensitive mutants. Nat Biotechnol. 2011;29(4):361–367.
Liang J, Xia L, Oyang L, Lin J, Tan S, Yi P, Han Y, Luo X, Wang H, Tang L, *et al.* The functions and mechanisms of prefoldin complex and prefoldin-subunits. Cell Biosci. 2020;10:1–15.
Loll-Krippleber R, Brown GW. P-body proteins regulate transcriptional rewiring to promote DNA replication stress resistance. Nat Commun. 2017;8(1):558.
Lopez-Fanarraga M, Avila J, Guasch A, Coll M, Zabala JC. Review: postchaperonin tubulin folding cofactors and their role in microtubule dynamics. J Struct Biol. 2001;135(2):219–229.
Machin NA, Lee JM, Barnes G. Microtubule stability in budding yeast: characterization and dosage suppression of a benomyl-dependent tubulin mutant. Mol Biol Cell. 1995;6(9):1241–1259.
Manders EMM, Stap J, Brakenhoff GJ, Van Driel R, Aten JA. Dynamics of three-dimensional replication patterns during the S-phase, analysed by double labelling of DNA and confocal microscopy. J Cell Sci. 1992;103(3):857–862.
Marnef A, Standart N. Pat1 proteins: a life in translation, translation repression and mRNA decay. Biochem Soc Trans. 2010;38(6): 1602–1607.
Martín-Benito J, Boskovic J, Gómez-Puertas P, Carrascosa JL, Simons CT, Lewis SA, Bartolini F, Cowan NJ, Valpuesta JM. Structure of eukaryotic prefoldin and of its complexes with unfolded actin and the cytosolic chaperonin CCT. EMBO J. 2002;21(23):6377–6386.
Millán-Zambrano G, Chávez S. Nuclear functions of prefoldin. Open Biol. 2014;4(7):140085.
Millán-Zambrano G, Rodríguez-Gil A, Peñate X, de Miguel-Jiménez L, Morillo-Huesca M, Krogan N, Chávez S. The prefoldin complex regulates chromatin dynamics during transcription elongation. PLoS Genet. 2013;9(9):e1003776.
Mitrea DM, Kriwacki RW. Phase separation in biology; functional organization of a higher order short linear motifs—the unexplored frontier of the eukaryotic proteome. Cell Commun Signal. 2016; 14:1–20.
Miyazawa M, Tashiro E, Kitaura H, Maita H, Suto H, Iguchi-Ariga SMM, Ariga H. Prefoldin subunits are protected from ubiquitin-proteasome system-mediated degradation by forming complex with other constituent subunits. J Biol Chem. 2011;286(22): 19191–19203.
Nissan T, Rajyaguru P, She M, Song H, Parker R. Decapping activators in *Saccharomyces cerevisiae* act by multiple mechanisms. Mol Cell. 2010;39(5):773–783.
Novotny I, Podolská K, Blazíková M, Valásek LS, Svoboda P, Stanek D. Nuclear LSm8 affects number of cytoplasmic processing bodies via controlling cellular distribution of Like-Sm proteins. Mol Biol Cell. 2012;23(19):3776–3785.
Oishi K, Kurahashi H, Pack CG, Sako Y, Nakamura Y. A bipolar functionality of Q/N-rich proteins: Lsm4 amyloid causes clearance of yeast prions. Microbiologyopen. 2013;2(3):415–430.
Parker R, Sheth U. P bodies and the control of mRNA translation and degradation. Mol Cell. 2007;25(5):635–646.
Pilkington GR, Parker R. Pat1 contains distinct functional domains that promote P-body assembly and activation of decapping. Mol Cell Biol. 2008;28(4):1298–1312.
Ramachandran V, Herman PK. Antagonistic interactions between the cAMP-dependent protein kinase and Tor signaling pathways modulate cell growth in *Saccharomyces cerevisiae*. Genetics. 2011; 187(2):441–454.
Ramachandran V, Shah KH, Herman PK. The cAMP-dependent protein kinase signaling pathway is a key regulator of P body foci formation. Mol Cell. 2011;43(6):973–981.
Reijns MA, Alexander RD, Spiller MP, Beggs JD. A role for Q/N-rich aggregation-prone regions in P-body localization. J Cell Sci. 2008; 121(Pt 15):2463–2472.
Richards KL, Anders KR, Nogales E, Schwartz K, Downing KH, Botstein D. Structure-function relationships in yeast tubulins. Mol Biol Cell. 2000;11(5):1887–1903.
Rippe K, Papantonis A. Functional organization of RNA polymerase II in nuclear subcompartments. Curr Opin Cell Biol. 2022;74:88–96.
Sachdev R, Hondele M, Linsenmeier M, Vallotton P, Mugler CF, Arosio P, Weis K. Pat1 promotes processing body assembly by enhancing the phase separation of the DEAD-box ATPase Dhh1 and RNA. eLife. 2019;8:e41415.
Sahin A, Daignan-Fornier B, Sagot I. Polarized growth in the absence of F-actin in *Saccharomyces cerevisiae* exiting quiescence. PLoS One. 2008;3(7):e2556.
Séraphin B. Sm and Sm-like proteins belong to a large family: identification of proteins of the U6 as well as the U1, U2, U4 and U5 snRNPs. EMBO J. 1995;14(9):2089–2098.
Shah KH, Nostramo R, Zhang B, Varia SN, Klett BM, Herman PK. Protein kinases are associated with multiple, distinct cytoplasmic granules in quiescent yeast cells. Genetics. 2014;198(4): 1495–1512.
Shah KH, Zhang B, Ramachandran V, Herman PK. Processing body and stress granule assembly occur by independent and differentially regulated pathways in *Saccharomyces cerevisiae*. Genetics. 2013;193(1):109–123.
Sheth U, Parker R. Decapping and decay of messenger RNA occur in cytoplasmic processing bodies. Science. 2003;300(5620):805–808.
Simons CT, Staes A, Rommelaere H, Ampe C, Lewis SA, Cowan NJ. Selective contribution of eukaryotic prefoldin subunits to actin and tubulin binding. J Biol Chem. 2004;279(6):4196–4203.
Sontag EM, Samant RS, Frydman J. Mechanisms and functions of spatial protein quality control. Annu Rev Biochem. 2017;86: 97–122.
Standart N, Weil D. P-bodies: cytosolic droplets for coordinated mRNA storage. Trends Genet. 2018;34(8):612–626.
Stoecklin G, Mayo T, Anderson P. ARE-mRNA degradation requires the 5'-3' decay pathway. EMBO Rep. 2006;7(1):72–77.
Sweet TJ, Boyer B, Hu W, Baker KE, Coller J. Microtubule disruption stimulates P-body formation. RNA. 2007;13(4):493–502.
Swisher KD, Parker R. Localization to, and effects of Pbp1, Pbp4, Lsm12, Dhh1, and Pab1 on stress granules in *Saccharomyces cerevisiae*. PLoS One. 2010;5(4):e10006.

Szymanski D. Tubulin folding cofactors: half a dozen for a dimer. Curr Biol. 2002;12(22):R767–769.

Teixeira D, Parker R. Analysis of P-body assembly in *Saccharomyces cerevisiae*. Mol Biol Cell. 2007;18(6):2274–2287.

Cleveland DW, Theodorakis NG. Regulation of Tubulin Synthesis. In: Hyams, Lloyd (editors). Microtubules; New York: Wiley-Liss, 1994. p. 47–58.

Thirumalai D, Lorimer GH. Chaperonin-mediated protein folding. Annu Rev Biophys Biomol Struct. 2001;30(1):245–269.

Toretsky JA, Wright PE. Assemblages: functional units formed by cellular phase separation. J Cell Biol. 2014;206(5):579–588.

Ursic D, Culbertson MR. The yeast homolog to mouse Tcp-1 affects microtubule-mediated processes. Mol Cell Biol. 1991;11(5): 2629–2640.

Vainberg IE, Lewis SA, Rommelaere H, Ampe C, Vandekerckhove J, Klein HL, Cowan NJ. Prefoldin, a chaperone that delivers unfolded proteins to cytosolic chaperonin. Cell. 1998;93(5):863–873.

van Dijk E, Cougot N, Meyer S, Babajko S, Wahle E, Séraphin B. Human Dcp2: a catalytically active mRNA decapping enzyme located in specific cytoplasmic structures. EMBO J. 2002;21(24): 6915–6924.

Vela-Corcía D, Romero D, De Vicente A, Pérez-García A. Analysis of β-tubulin-carbendazim interaction reveals that binding site for MBC fungicides does not include residues involved in fungicide resistance. Sci Rep. 2018;8(1):12.

Weinstein B, Solomon F. Phenotypic consequences of tubulin overproduction in *Saccharomyces cerevisiae*: differences between alpha-tubulin and beta-tubulin. Mol Cell Biol. 1990;10(10):5295–5304.

Xing W, Muhlrad D, Parker R, Rosen MK. A quantitative inventory of yeast P body proteins reveals principles of composition and specificity. eLife. 2020;9:1–63.

Zhang B, Butler AM, Shi Q, Xing S, Herman PK. P-body localization of the Hrr25/casein kinase 1 protein kinase is required for the completion of meiosis. Mol Cell Biol. 2018;38(17):e00678–00617.

Zhang B, Herman PK. It is all about the process(ing): p -body granules and the regulation of signal transduction. Curr Genet. 2020;66(1): 73–77.

Zhang B, Shi Q, Varia SN, Xing S, Klett BM, Cook LA, Herman PK. The activity-dependent regulation of protein kinase stability by the localization to P-bodies. Genetics. 2016;203(3):1191–1202.

Zid BM, O'Shea EK. Promoter sequences direct cytoplasmic localization and translation of mRNAs during starvation in yeast. Nature. 2014;514(7520):117–121.

Communicating editor: A. Mitchell